

From prosumer to flexumer: Case study on the value of flexibility in decarbonizing the multi-energy system of a manufacturing company

Markus Fleschutz^{a,b}, Markus Bohlayer^a, Marco Braun^a, Michael D. Murphy^b

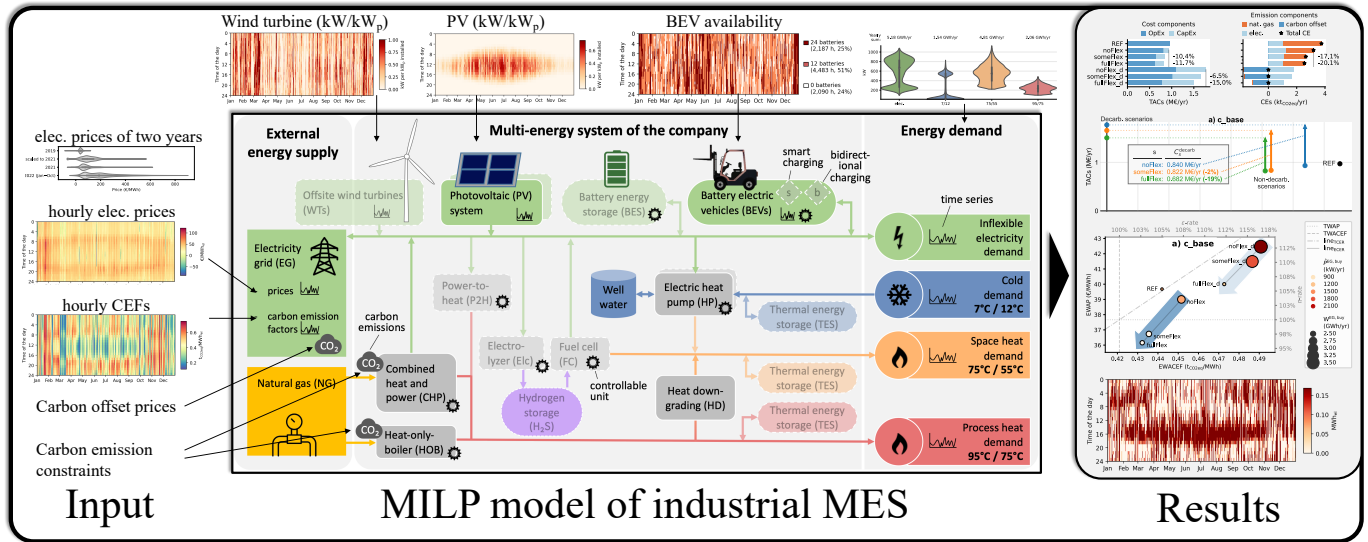
^aInstitute of Refrigeration, Air-Conditioning, and Environmental Engineering, University of Applied Sciences Karlsruhe, Moltkestraße 30, 76133 Karlsruhe, Germany

^bDepartment of Process, Energy and Transport Engineering, Munster Technological University, Bishopstown, Cork, Ireland

Abstract

Digitalization and sector coupling enable companies to turn into flexumers. By using the flexibility of their multi-energy system (MES), they reduce costs and carbon emissions while stabilizing the electricity system. However, to identify the necessary investments in energy conversion and storage technologies to leverage demand response (DR) potentials, companies need to assess the value of flexibility. Therefore, this study quantifies the flexibility value of a production company's MES by optimizing the synthesis, design, and operation of a decarbonizing MES considering self-consumption optimization, peak shaving, and integrated DR based on hourly prices and carbon emission factors (CEFs). The detailed case study of a beverage company in northern Germany considers vehicle-to-X of powered industrial trucks, power-to-heat on multiple temperatures, wind turbines, photovoltaic systems, and energy storage systems (thermal energy, electricity, and hydrogen). We propose and apply novel data-driven metrics to evaluate the intensity of price-based and CEF-based DR. The results reveal that flexibility usage reduces decarbonization costs (by 19–80% depending on electricity and carbon removal prices), total annual costs, operating carbon emissions, energy-weighted average prices and CEFs, and fossil energy dependency. The results also suggest that a net-zero operational carbon emission MES requires flexibility, which, in an economic case, is provided by a combination of different flexible technologies and storage systems that complement each other. While the value of flexibility depends on various market and consumer-specific factors such as electricity or carbon removal prices, this study highlights the importance of demand flexibility for the decarbonization of MESs.

arXiv:2301.07997v1 [eess.SY] 19 Jan 2023



Keywords: Energy flexibility, Demand response, Multi energy system, Hourly carbon emission factors, Distributed energy resources, Flexibility metrics, Decarbonization

Highlights

- Detailed case study of optimal net-zero multi-energy system design using MILP.
- Quantified the flexibility value of an distributed energy system for decarbonization.
- Novel metrics to evaluate price-based and emission-based demand response.
- Considered power-to-hydrogen, vehicle-to-X, and multi-temperature power-to-heat.
- Compare the value of using existing versus new flexibility.
- Flexibility of distributed energy resources reduced decarbonization costs by 19–80%.

Email address: michael.d.murphy@mtu.ie (Michael D. Murphy)

Nomenclature

Acronyms / abbreviations / superscripts

BES	Battery energy storage
BEV	Battery electric vehicle
C&I	Commercial and industrial
CapEx	Capital expenditures
capx/capn	Nominal capacity of existing/new assets
CE	Carbon emission
CEF	Carbon emission factor
CHP	Combined heat and power
cond	Condensation
COP	Coefficient of performance
DAC	Direct air capture
DR	Demand response
DRAF	Demand Response Analysis Framework
ECER	Energy-based cost-emission ratio
EG	Electricity grid
Elc	Electrolyzer
elec	Electricity
eva	Evaporation
EWACEF	Energy-weighted average carbon emission factor
EWAP	Energy-weighted average price
FC	Fuel cell
H ₂	Hydrogen
H ₂ S	Hydrogen storage
HD	Heat downgrading
HOB	Heat-only boiler
HP	Electrical heat pump
inv	Investment
KPI	Key performance indicator
MEF	Marginal emission factor
MES	Multi-energy system
MILP	Mixed-integer linear programming
NF	Network fees
NG	Natural gas
OC	Own-consumption

OpEx	Operating expenses
P2H	Power-to-heat
PV	Photovoltaic
RMI	Repair, maintenance, and inspection
TAC	Total annualized cost
TCER	Time-based cost-emission ratio
TES	Thermal energy storage
TWACEF	Time-weighted average carbon emission factor
TWAP	Time-weighted average price
V2X	Vehicle-to-everything
vRES	Variable renewable energy source
WT	Wind turbine
XEF	Grid-mix emission factor

Indices / sets

$b \in \mathcal{B}$	Types of battery electric vehicle
$c \in \mathcal{C}$	Condensing temperature levels
$h \in \mathcal{H}$	Heating temperature levels
$i \in \mathcal{I}$	Technology components
$n \in \mathcal{N}$	Cooling temperature levels
$t \in \mathcal{T}$	Time steps

Symbols

\dot{Q}	Thermal energy flow
η	Efficiency coefficient
γ	Coefficient related to capacity
$\pi_s, \varepsilon_s, \omega_s$	Normalized flexibility metrics
ε	Specific carbon emissions
c	Specific costs
C, c	Annual/specific costs
E	Electrical energy
n	Economic life in years
P	Electrical power
R	Annual revenue
r	Discount rate
Y, y	Binary variable
z	Switch for flexibility or investment option

1. Introduction

1.1. Motivation

In the course of the European Green Deal [1], the European Union is aiming for climate neutrality by 2050. As an interim target, a 55% carbon emission (CE) reduction by 2030 compared to 1990 levels was set. According to the Emissions Gap Report 2021 of the United Nations Environment Programme [2], these targets are not sufficient to meet the 1.5 °C target of the Paris Agreement. However, they are still ambitious and just one example of the global pursuit of deep decarbonization.

To meet these challenging targets and to stay within sustainable biomass limits, a high degree of electrification and hydrogen (H₂) integration is needed in the energy system [3] and the industry sector [4]. Sector coupling such as the electrification of heat and mobility enables sectors that traditionally relied on fossil fuels, to benefit from the decarbonization possibilities of the electricity sector, e.g. photovoltaic (PV) and wind power [5]. In turn, the sector coupling allows transferring operational flexibility from other energy sectors (heat, mobility,

H₂) to the electricity sector [6]. This operational flexibility is necessary to compensate for the increasing shares of fluctuating renewable energy and the decommissioning of controllable thermal power plants. Thus, carbon-free electricity systems require four times the operational flexibility of conventional systems [7]. Demand response (DR) programs activate demand-side flexibility through different incentive systems. Electrification gives rise to multi-energy systems (MESs) that can provide existing and newly created flexibility that can be used through DR [8]. Besides private households and heavy industry, also the commercial and industrial (C&I) sector exhibits so far untapped flexibility potential [9].

By untapping demand-side flexibility potentials, an electricity prosumer turns into a “flexumer” [10]. While a prosumer draws power from the grid and feeds in surpluses, a flexumer additionally controls the energy profiles through smart use of energy conversion and storage technologies. Fig. 1 illustrates a comparison of the terms consumer, prosumer, and flexumer.

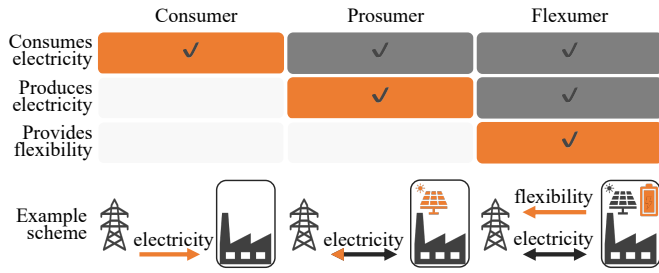


Fig. 1. Differentiation of the terms consumer, prosumer, and flexumer.

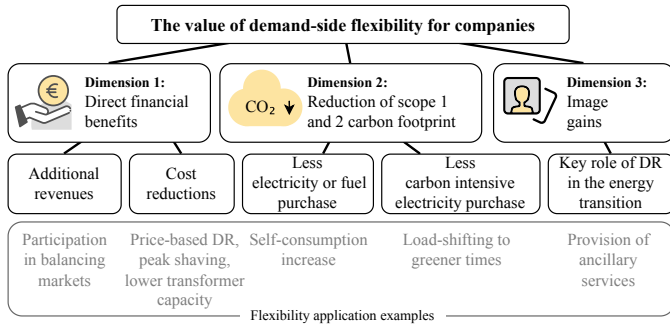


Fig. 2. The value of demand-side flexibility for companies.

1.2. Background

Despite the worldwide expansion of variable renewable energy sources (vRESs), the wholesale electricity prices of the last decades offered few incentives for flexibility [12]. However, since the second half of the year 2021, European electricity prices skyrocketed as a result of increased carbon and fuel prices. The natural gas price were especially driven by the COVID-19 pandemic and the Russian invasion of Ukraine, but also by technical issues, longer winter, and lower wind and hydro generation [13]. Additionally, in countries with substantial vRES shares, not only the level of wholesale electricity prices has increased, but also the price fluctuation due to the merit order effect [14]. For example, in Germany, mean daily price spreads (i.e., difference between lowest and highest price of each day) increased almost ten-fold between 2019 and 2022, see Fig. 3. Interestingly, in 2022, on average, the daily price spread were 1.37x the price itself which means that the load shift of a unit of energy from the most expensive hour of the day to the cheapest paid for the average generation of 1.37 times that energy.

Despite the existence of fixed electricity price components such as network charges and taxes that hinder flexibility, demand-side energy flexibility can provide value for the electricity system but also for companies [15]. There are several flexibility applications, e.g., ancillary service provision, energy-only market optimization, peer-to-peer energy trading, congestion management, self-consumption optimization, and peak-shaving [16, 17]. The value of demand-side flexibility for a company can be divided into three dimensions, see Fig. 2. Dimension 1 is direct financial benefits through additional revenue streams or cost reductions. Dimension 2 represents the reduction of the company's Scope I and II carbon footprint by reducing the purchased energy's volume or carbon-intensity or both. Dimension 3 includes

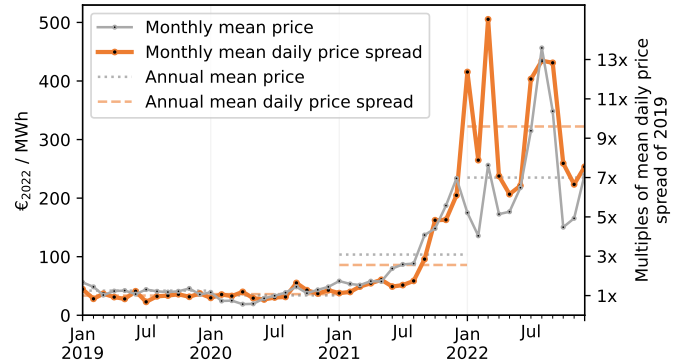


Fig. 3. Day-ahead spot market prices and daily price spreads of Germany and Luxembourg for 2019–2022. Prices sourced from [11].

corporate image gains, since DR helps stabilize the electricity system, prevents blackouts, and integrates vRESs in the electricity system [18]. With increasing renewable energy shares, DR and energy flexibility in general will gain reputation as key components of the energy transition [19]. By participating in DR, production companies provide an important overarching contribution that they can publicly communicate [20]. Note that the environmental and the financial benefits may interact, e.g., financial benefits (Dimension 1) could finance clean technologies and reduce carbon footprint. Analogously, carbon footprint reductions (Dimension 2) may reduce the need for expensive carbon removal and, therefore, imply financial benefits.

1.3. Literature review

There is a growing body of literature that evaluate the potentials from demand-side flexibility. Muche et al. [21] used mixed-integer linear programming (MILP) to analyze the revenue of participation of combined heat and power (CHP) plants in control reserve markets. In [22], an intelligent energy management framework based on MILP with DR capability was proposed for industrial facilities. Besides thermostatically controlled loads and battery electric vehicles (BEVs) also production processes and renewable generation were analyzed. However, in both studies, CEs were not considered. Kelley et al. [23] used MILP to model DR of air separation units. They provided a novel scheduling framework that accounts for plant dynamics, however, only focussing on one DR application. Scholz et al. [24] analyzed the energy flexibility of forklift trucks within a MES but without considering investment decisions or vehicle-to-everything (V2X).

Summerbell et al. [25] studied the cost and CE reduction potentials of a cement plant through price-based DR using real-time pricing. The CE reduction potential was calculated from dynamic CEFs, however, investments were not considered. A scheduling simulation resulted in electricity costs and electricity-derived CE reductions of 4% each. Alabi et al. [26] proposed a multi-objective design and operation optimization model for carbon neutral MESSs. In a case study, they analyzed the effects of considering energy storage aging and DR. However, the methodology was not applied to the C&I sector but to a residential district in Hong Kong. Ahmarinejad [27], presented a

multi-objective planning and operation MILPs model considering DR. However, in contrast to our study, DR was not evaluated in a real-world case study. Petkov and Gabrielli [28] presented a multi-objective design optimization formulation for MESs considering H₂ as a seasonal energy storage. They concluded that for valid seasonal storage evaluations, optimization must be performed over at least 2,000 hourly resolved time steps. Also the results indicated that a MES can only reach net zero operational CEs using power-to-H₂. Mansouri et al. [29] proposed an investment and operation optimization framework for MES considering DR. The results indicate a 15.1% reduction of operating expenses (OpEx) through price-based load shifting. However, only Scope I CEs were considered and with fixed carbon emission factors (CEFs). In [30], a design and operation optimization MILP problem was formulated and applied to the data of an exhibition center in south Italy. Energy flexibility was considered through peak shaving with a BES. CEs were assessed, but only with annual CEFs, and carbon neutrality was not analyzed. Baumgärtner et al. [31] proposed an optimal planning and operation model considering hourly CEFs, price-based DR and carbon neutrality. Costs and CEs were calculated comparing the use of annual versus hourly CEFs. The significant differences in resulting costs and CEs highlight the importance of hourly CEFs. The model was applied within a real-world case study of a chemical industry MES. However, the value of flexibility was not explicitly quantified. Furthermore, Jordehi [32] concluded a comprehensive review on DR that more research effort should be placed on the C&I sector, on more realistic optimization problems, and the analysis of environmental effects.

Recently several studies proposed flexibility metrics to quantify and characterize price-based DR. In [10], four metrics (price responsiveness score, consistency score, flexible amount, and response time score) were proposed to identify and classify flexusers based on their electricity price and load. However, CEFs were not considered and the metrics were not designed with real-time pricing in mind but with time-of-use tariffs. Zhengyi et al. [33] reviewed DR quantification indicators for residential energy flexibility and classified them into direct and indirect indicators. While direct indicators are directly related to the features of a building, indirect indicators also consider economic and environmental factors. The mentioned indirect indicators are operation cost savings, operation cost reduction ratio, cost flexibility factor and carbon emission reductions. However weighted averages based on electricity price and load are not mentioned. The carbon emission reduction indicator is based on time-independent CEFs. In [34], several flexibility metrics are proposed, however, focusing only on incentive-based DR, so they cannot be applied to price or CEF-based DR. Very recently, this study [35] reviewed 156 articles and identified 48 data-driven energy flexibility key performance indicators (KPIs) for operational buildings. The KPIs could be grouped based on whether a baseline energy demand (penalty-ignorant operation) is required. For baseline-required KPIs, building performance data in both flexible and reference scenarios are necessary, while baseline-free KPIs can be calculated without a reference scenario. Also, the development of new baseline-free KPIs and the consideration of non-engineering factors such as costs and

CEs was identified as major research gaps. The energy-weighted average electricity price – mostly referred to as load-weighted or demand-weighted average price – is a wide-spread metric, e.g., used in [36, 37, 38]. However, to the best of the authors’ knowledge, it has been used in the context of large-scale electricity systems and not to evaluate the DR intensity of local MESs. Demand-weighted CEFs, in contrast, have only been used since hourly CEFs became widely available [39]. However, in this study, we use energy-weighted average electricity prices to evaluate the effectiveness of price-based and CEF-based DR of an industrial company’s MES and to compare it between scenarios.

In summary, the inclusion and evaluation of energy flexibility are gaining interest also for the C&I sector. However, the presented studies often do not consider investments, dynamic CEFs, or carbon neutrality as we do. Others do not explicitly evaluate DR with metrics designed for this purpose. Thus, to the best of the authors’ knowledge, no study evaluates the flexibility of a production company’s MES in a detailed case study considering investments and evaluating price-based and CEF-based DR under carbon neutrality conditions. Also, there is a lack of studies on the development of metrics to evaluate price-based and CEF-based DR.

1.4. Study contribution

In this paper, we quantify the value of existing and new flexibility of a production company’s MES in the context of decarbonization. To this end, we apply a synthesis, design, and operation optimization MILP model to the real-world data of a beverage plant in Germany for different scenarios and contexts. We propose and apply several flexibility metrics to evaluate DR based on prices and hourly CEFs. The detailed case study considers H₂ storage, hourly electricity CEFs and prices, power-to-mobility, power-to-heat on multiple temperature levels and more and focuses on the flexibility applications self-consumption optimization, price-based and CEF-based voluntary DR, and peak shaving.

The remainder of this paper is organized as follows. We first explain the case study in Section 2. Subsequently, the optimization model is described in Section 3 and the evaluation metrics defined in Section 4. The scenarios and contexts are defined in Section 5 before we present and discuss the results of the analysis in Section 6. Finally, we conclude in Section 7.

2. Case study

We consider the MES of a beverage company in northern Germany. Fig. 4 shows a schematic depiction of the case study. This company has already invested in renewable infrastructure and is working towards carbon neutrality.

2.1. Energy demands

The company has an electricity demand and three different thermal energy demands with the following flow/return temperature levels in °C: Cooling demand (7/12), space heat demand (75/55), and process heat demand (95/75). We calculated the

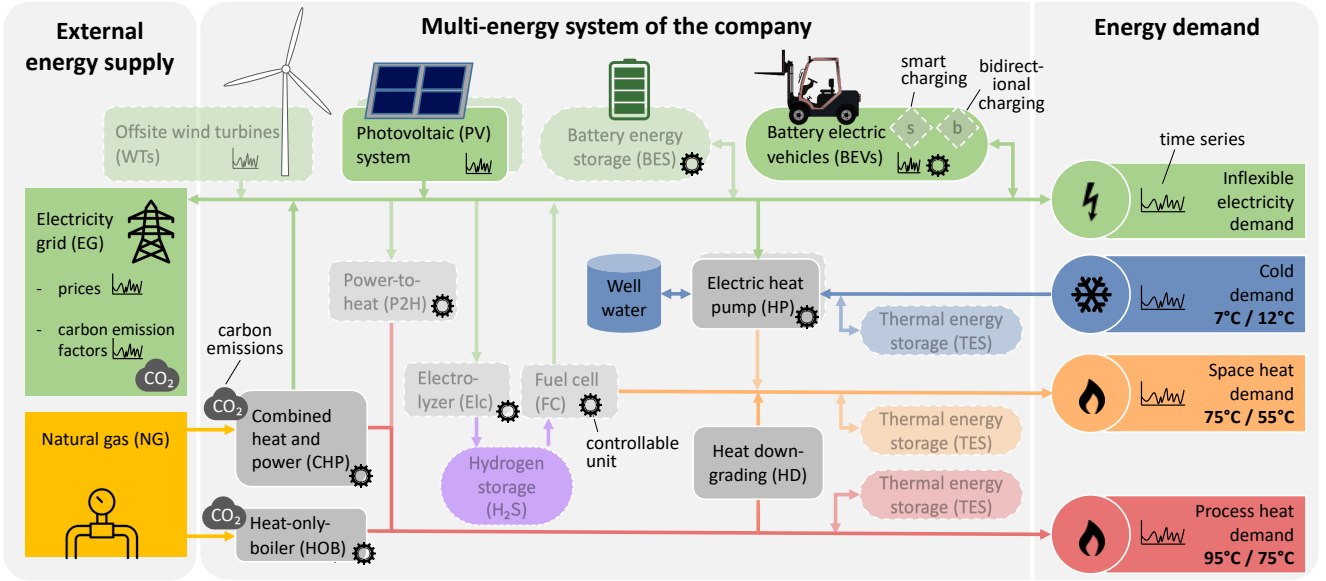


Fig. 4. Overview scheme of the case study. It shows the external energy supply (left), the company's multi-energy system (MES) (center) including conversion and storage technologies, the energy demand of the company (right), and the energy flows between the components. Greyed-out energy flows or components such as the thermal energy storage (TES) or the power-to-heat (P2H) do currently not exist but are possible to implement. In the status quo of the MES, the electricity demand is provided by a photovoltaic (PV) system, a combined heat and power (CHP) system based on natural gas, and the electricity grid (EG). There are no energy storage systems except the battery electric vehicles (BEVs) but they are charged unidirectionally with full power until full. The cold demand is served by the cooling machine (electric heat pump (HP) without using the hot side to serve heat demands). The heat demands on both temperature levels are met by the CHP and a natural gas fueled heat-only boiler (HOB).

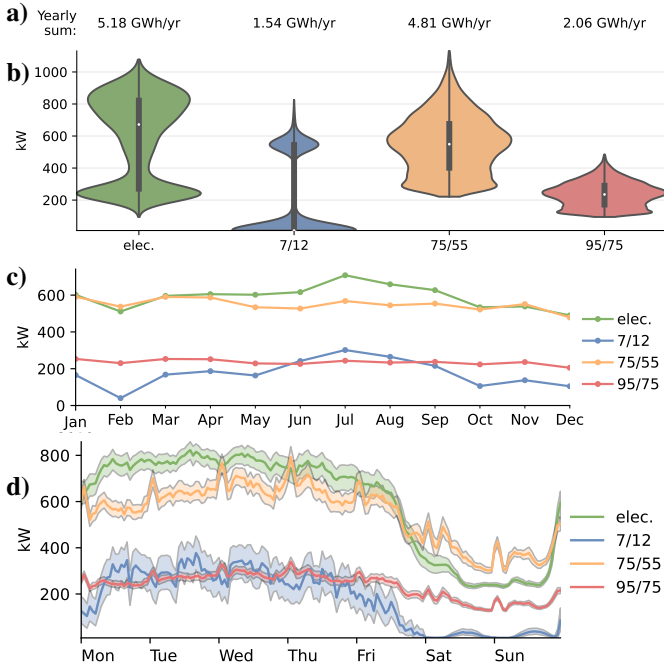


Fig. 5. Description of the electricity (elec.) and thermal energy (75/55, 95/75, 7/12) demand time series. **a)** Annual energy sums, **b)** violin plots showing annual distribution, **c)** monthly average demand, **d)** average week and 95% confidence interval.

hourly inflexible electricity demand that is independent of flexible operation and stays the same for all scenarios:

$$P_t^{\text{eDem}} = \tilde{P}_t^{\text{EG,buy}} + \tilde{P}_t^{\text{PV,OC}} - \tilde{P}_t^{\text{BEV,drive}} - \tilde{P}_t^{\text{CM}} \quad \forall t \in \mathcal{T} \quad (1)$$

where $\tilde{P}_t^{\text{EG,buy}}$, $\tilde{P}_t^{\text{PV,OC}}$, and $\tilde{P}_t^{\text{BEV,drive}}$ are the historic data for the purchased electricity from the electricity grid (EG), the PV energy consumed from the onsite PV system, and the electricity consumption of the BEVs, respectively. \tilde{P}_t^{CM} is an approximation of the cooling machine. Fig. 5 presents key metrics of the three thermal demands and the inflexible electricity demand. It can be seen that the cold demand has a seasonal pattern peaking in summer, while the heat demands are more stable throughout the year. Electricity demand is slightly higher during the summer months due to the increased beverage production.

2.2. Existing technologies

The company runs an onsite 307 kW_p PV system. For the analyses, we used the historic measured electricity generation of the year 2019, see Section 3.4.1. Based on available roof space, an additional PV capacity of up to 2,770 kW_p can be built with the same profile and efficiency. A cooling machine with 860 kW cooling power exists on site that can recool with 10°C well water. The company owns a CHP with 410 kW_{th} nominal heating power and a 1,620 kW_{th} heat-only boiler (HOB). Both run on natural gas and supply heat on the 97/75 temperature level. There are 24 Li-ion industrial truck batteries with a net capacity of 81.1 kWh each.

3. Optimization model

3.1. Overview

To quantify the value of flexibility for this company, we formulate a deterministic MILP using technology components of version v0.3.0 [40] of the open-source Python Demand Response

Analysis Framework (DRAF), a modular tool for economic and environmental evaluation of DR [41]. An overview of the model is shown in Fig. 6. DRAF and most used technology components are detailed in [41]. However, model parts that are crucial (cost and carbon balances, HP, BEV) or not described in [41] such as wind turbine (WT), pressurized H₂ storage (H₂S), proton exchange membrane fuel cell (FC), proton exchange membrane electrolyzer (Elc), and direct air capture (DAC) are described in this section.

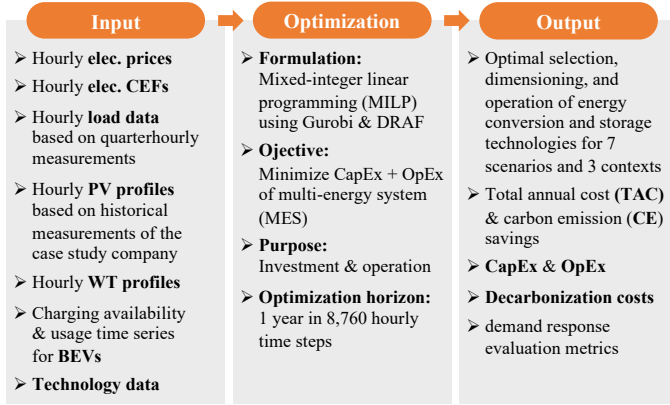


Fig. 6. Main technical model features

We model one year with 8,760 hourly time steps $t \in \mathcal{T}$, so $\Delta t = 1$ h. We assume perfect foresight. Optimization variables are indicated in bold and are non-negative continuous variables if not specified.

The objective function of the MILP problem is the minimization of the total annualized cost (TAC) in k€/yr and the penalty term X^{penalty} to model conventional charging. The TAC include capital expenditures (CapEx) and operating expenses (OpEx), see Eq. (3).

$$\text{minimize } \mathbf{TAC} + X^{\text{penalty}} \quad (2)$$

$$\mathbf{TAC} = \mathbf{CapEx} + \mathbf{OpEx} \quad (3)$$

$$\mathbf{TAC}, \mathbf{OpEx} \in \mathbb{R}$$

The CapEx represent the annualized investment costs for all technical components in the technology set \mathcal{I} :

$$\mathbf{CapEx} = \sum_{i \in \mathcal{I}} a(r, n_i) c_i^{\text{inv}} P_i^{\text{capn}} \quad (4)$$

where c_i^{inv} are the specific investment costs and P_i^{capn} the new nominal capacity of technology $i \in \mathcal{I}$. $a(r, n_i)$ is the annuity factor of component i as function of the discount rate r and the economic life n_i in years, see Eq. (5).

$$a(r, n_i) = \frac{r(1+r)^{n_i}}{(1+r)^{n_i} - 1} \quad (5)$$

The OpEx represent the operating costs of the first year

$$\begin{aligned} \mathbf{OpEx} = & C^{\text{RMI}} + C^{\text{EG,buy}} - R^{\text{EG,sell}} + C^{\text{EG,NF}} \\ & + C^{\text{WT,NF}} + C^{\text{NG}} + C^{\text{NG,tax}} + C^{\text{DAC}} \end{aligned} \quad (6)$$

$$C^{\text{EG,sell}}, C^{\text{EG,sell}} \in \mathbb{R}$$

where C^{RMI} are the repair, maintenance, and inspection (RMI) costs, $C^{\text{EG,buy}}$ are the costs of purchased electricity, $R^{\text{EG,sell}}$ are the revenue of sold electricity, $C^{\text{EG,NF}}$ and $C^{\text{WT,NF}}$ are the network fees of purchased electricity and self-consumed electricity from the WT, respectively, C^{NG} are the costs of purchased natural gas, $C^{\text{NG,tax}}$ are the carbon tax costs due to the purchased natural gas, and C^{DAC} are the costs for carbon removal.

The total operating CEs of the first year are calculated through:

$$\begin{aligned} \mathbf{CE} = & \underbrace{\Delta t \varepsilon^{\text{NG}} \sum_{t \in \mathcal{T}} P_t^{\text{NG,buy}}}_{\text{Scope I (direct)}} + \underbrace{\Delta t \sum_{t \in \mathcal{T}} \varepsilon_t^{\text{elec}} P_t^{\text{EG,buy}}}_{\text{Scope II (indirect)}} - \underbrace{\mathbf{CE}^{\text{DAC}}}_{\text{carbon removal}} \end{aligned} \quad (7)$$

where ε^{NG} is the CEF for natural gas, $\varepsilon_t^{\text{elec}}$ denote the hourly electricity CEFs, and \mathbf{CE}^{DAC} are the removed CEs.

3.2. Electricity grid (EG)

Electricity tariff. We used historic hourly day-ahead electricity prices c_t^{elec} of the year 2019 ($c_t^{\text{elec},2019}$), as shown in Fig. 7 top, which were sourced from the ENTSO-E transparency platform [11] via the Python package *elmada* [42]. The purchased electricity $P_t^{\text{EG,buy}}$ is limited to $P^{\text{EG,buy,max}}$ of 20 MW and evaluated with a real-time pricing tariff consisting of c_t^{elec} and a fixed price add-on $c^{\text{EG,addon}}$ of €62.28 MWh⁻¹ for taxes and levies, see Eqs. (8) and (9). Additionally, €70 fixed network fees $\hat{c}^{\text{EG,buy}}$ are charged per kW of the highest demand of the year $\hat{P}^{\text{EG,buy}}$, see Eq. (10). The sold electricity $P_t^{\text{EG,sell}}$ is limited to $P^{\text{EG,sell,max}}$ of 20 MW and compensated with c_t^{elec} , see Eqs. (11) and (12).

$$C^{\text{EG,buy}} = \Delta t \sum_{t \in \mathcal{T}} P_t^{\text{EG,buy}} (c_t^{\text{elec}} + c^{\text{EG,addon}}) \quad (8)$$

$$P_t^{\text{EG,buy}} \leq \hat{P}^{\text{EG,buy}} \leq P^{\text{EG,buy,max}} \quad \forall t \in \mathcal{T} \quad (9)$$

$$C^{\text{EG,NF}} = \hat{P}^{\text{EG,buy}} \hat{c}^{\text{EG,buy}} \quad (10)$$

$$R^{\text{EG,sell}} = \Delta t \sum_{t \in \mathcal{T}} P_t^{\text{EG,sell}} c_t^{\text{elec}} \quad (11)$$

$$P_t^{\text{EG,sell}} \leq P^{\text{EG,sell,max}} \quad \forall t \in \mathcal{T} \quad (12)$$

Electricity carbon emission factors (CEFs). National dynamic electricity grid-mix CEFs (XEFs), shown in Fig. 7 bottom, were calculated using the XEF_EP method of *elmada* [42]. This method uses fuel type-specific generation data from the ENTSO-E transparency platform [11] and fuel type-specific CE intensities from [43]. Electricity purchased from the EG was evaluated with XEFs, while the negative CEs through grid feed-in from own vRESs were not compensated.

Our analysis includes short-term load shifting, for which marginal emission factors (MEFs) should be used as demonstrated in [44] if the impact on CEs is explicitly examined. However, since the environmental DR potentials in this analysis are modeled implicitly and inseparable from the investment decisions we take an attributional approach, thus using XEFs for $\varepsilon_t^{\text{EG}}$.

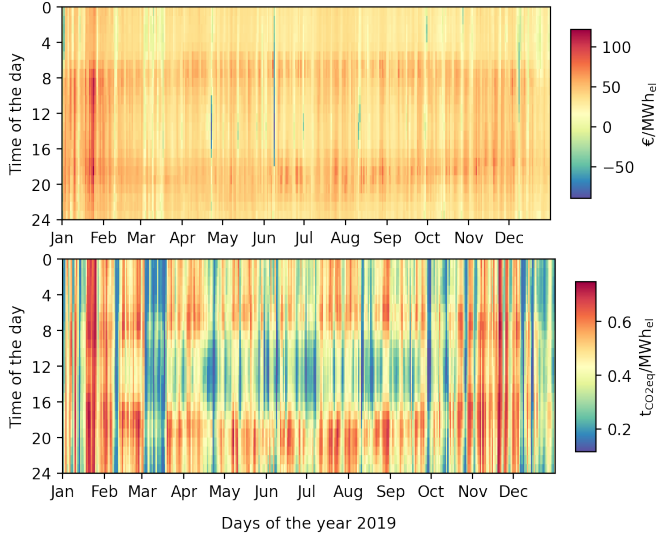


Fig. 7. Day-ahead spot market prices ($c_t^{\text{elec},2019}$, top) and XEFs ($\varepsilon_t^{\text{elec}}$, bottom) for the German electricity market of the year 2019.

3.3. Natural gas grid

Natural gas can be purchased for $\text{€}43 \text{ MWh}^{-1}$ with $0.240 \text{ t}_{\text{CO}_2\text{eq}}/\text{MWh}$ [45] carbon emission intensity. Additionally, a carbon tax $c^{\text{NG,tax}}$ of $\text{€}55 \text{ t}_{\text{CO}_2\text{eq}}^{-1}$ has to be paid.

3.4. Technologies

Fig. 12 depicts the conversion and storage technologies used in our case study and an overview of their main parameters is given in Table 1.

3.4.1. Conversion technologies

The conversion technologies CHP, Elc, FC, HOB, and P2H are modeled with a linear input-output relationship

$$P_t^{\text{in}} = \eta P_t^{\text{out}} \quad \forall t \in \mathcal{T} \quad (13)$$

$$P_t^{\text{out}} \leq P^{\text{cap}} \quad \forall t \in \mathcal{T} \quad (14)$$

where some technologies have multiple outputs, see also Table 1.

Electrical heat pump (HP). The HP has two heat sources $n \in \mathcal{N}$ (cold demand with 7°C and the well water with 10°C) and two heat sinks $c \in \mathcal{C}$ (the well water and the space heat demand with 75°C). This results in three possible combinations of source-sink temperature levels defining the operating mode: Cold demand to well, cold demand to heat demand, and well to heat demand. The coefficient of performance (COP) is calculated for each time step t and operating mode:

$$\text{COP}_{t,c,n}^{\text{HP}} = \eta^{\text{HP,Carnot}} \underbrace{\frac{\vartheta_{t,c}^{\text{HP,cond}} + 273.15}{\vartheta_{t,c}^{\text{HP,cond}} - \vartheta_{t,n}^{\text{HP,eva}}}}_{\text{COP}_{\text{Carnot}}} \quad \forall t \in \mathcal{T}, c \in \mathcal{C}, n \in \mathcal{N}. \quad (15)$$

The evaporation and condensation temperatures ($\vartheta_{t,n}^{\text{HP,eva}}$, $\vartheta_{t,c}^{\text{HP,cond}}$) were calculated assuming a 5°C temperature difference to consider heat exchange for both evaporator and condenser. Following [54], a decision variable $Y_{t,c,n}^{\text{HP}}$ is used to select the operating mode. Multiple HPs are considered if $n^{\text{HP,modes}} > 1$:

$$\dot{Q}_{t,c,n}^{\text{HP}} \leq Y_{t,c,n}^{\text{HP}} \dot{Q}^{\text{HP,max}} \quad \forall t \in \mathcal{T}, c \in \mathcal{C}, n \in \mathcal{N} \quad (16)$$

$$\sum_{c \in \mathcal{C}} \sum_{n \in \mathcal{N}} Y_{t,c,n}^{\text{HP}} \leq n^{\text{HP,modes}} \quad \forall t \in \mathcal{T} \quad (17)$$

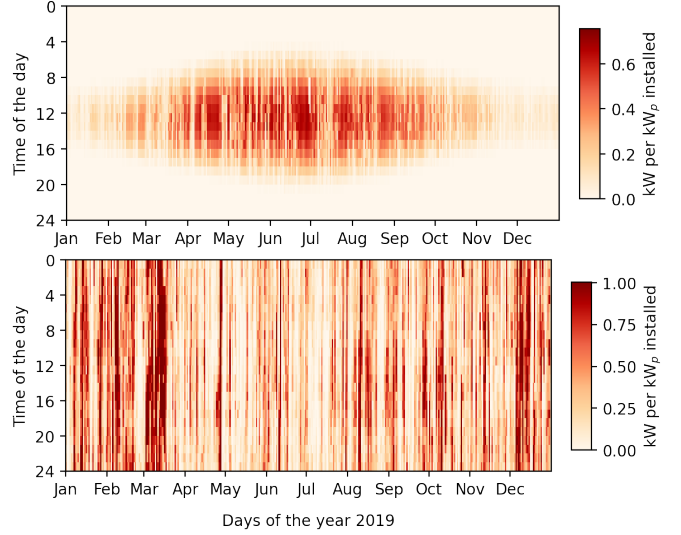


Fig. 8. Historic electricity generation profile per kW_p installed capacity of the case study PV system (top) and the Kelmarsh 6 WT (bottom).

Photovoltaic (PV). The PV electricity generation time series per kW_p installed capacity is an exogenous variable. We used historic measurements of the case study company for the year 2019 in an aggregated form, see Fig. 8 top. The capacity factor for 2019 is 0.10.

Wind turbine (WT). The wind electricity generation time series per kWh_p installed capacity is an exogenous variable, see Fig. 8 bottom. The hourly profile for 2019 is aggregated from the open data of the Kelmarsh 6 [55], a 2.04 MW Senvion MM92 WT located in the Kelmarsh wind farm in the United Kingdom which is used as a proxy for northern Germany. The capacity factor for 2019 is 0.33. For used WT electricity, an electricity price addon $c^{\text{EG,addon}}$ is paid. Unused WT electricity is sold at the day-ahead market price assuming that the guarantees of origins are sold for a negligible price, so there are no negative CEs. Investment in partial WTs (shareholder) are possible.

3.4.2. Storage technologies

Battery energy storage (BES). The constraints for the BES are:

$$\begin{aligned} \mathbf{E}_t = \eta^{\text{time}} & \begin{cases} k^{\text{ini}} \mathbf{E}^{\text{capn}} & \text{if } t = t_0 \\ \mathbf{E}_{t-1} & \text{otherwise} \end{cases} \\ & + \Delta t \left(\eta^{\text{ch}} \mathbf{P}_t^{\text{in}} - \frac{\mathbf{P}_t^{\text{out}}}{\eta^{\text{dis}}} \right) \quad \forall t \in \mathcal{T} \end{aligned} \quad (18)$$

Table 1
Technology parameters

Technology	Specific inv. costs c^{inv} (€/base)	Base	RMI costs c^{RMI} (%/yr)	Economic life n (yr)	Input	Efficiency η (%)	Output	C rate λ (kW/kWh)	
Conversion	CHP	589.46 [46]	kW _{el}	18	25	natural gas	40	elec.	-
	—	-	-	-	-	natural gas	45	heat	-
	Elc ^b	1,295 [28]	kW _{el}	3.8	14	elec.	71	H ₂	-
	FC ^b	1,684 [28]	kW _{el}	3.8	14	H ₂	50	elec.	-
	—	-	-	-	-	H ₂	34	heat	-
	HOB	57.13 [47]	kW _{th}	18	15	natural gas	90	heat	-
	HP	387 [28]	kW _{th,cond}	2.5	18	elec., heat	50 ^b	heat	-
	P2H	100 [48]	kW _{th}	0	30	elec.	90	heat	-
Storage	PV	460 [49]	kW _p	2	25	- given profile -	-	elec.	-
	WT	1,682 [50]	kW _p	1	20	- given profile -	-	elec.	-
	BES	600 [51]	kWh _{el}	2	20	elec.	95 _{cycle} ^c	elec.	0.7
	BEV	-	-	-	-	elec.	95 _{cycle}	elec.	0.7
	H ₂ S	10 [28]	kWh _{H₂}	0	23	H ₂	90 _{cycle}	H ₂	- ^d
	TES	28.71 [52]	kWh _{th}	0.1	30	heat	99.5 _{time}	heat	0.5

^a Based on investment costs

^b Exergy efficiency $\eta^{\text{HP,Carnot}}$ (ratio of reaching ideal Carnot COP)

^c Additionally, $\eta^{\text{time}}=99.998\%$ applies every hour due to self-discharge [53]

^d The C rate of H₂S is determined by the Elc and FC capacities.

$$\mathbf{P}_t^{\text{in}} \leq \lambda^{\text{in}} \mathbf{E}^{\text{capn}} \quad \forall t \in \mathcal{T} \quad (19)$$

$$\mathbf{P}_t^{\text{out}} \leq \lambda^{\text{out}} \mathbf{E}^{\text{capn}} \quad \forall t \in \mathcal{T} \quad (20)$$

$$\mathbf{E}_t \leq \mathbf{E}^{\text{capn}} \quad \forall t \in \mathcal{T} \quad (21)$$

$$\mathbf{E}_{t_{\text{ref}}} = k^{\text{ini}} \mathbf{E}^{\text{capn}} \quad (22)$$

Hydrogen storage (H₂S) and thermal energy storage (TES). H₂S and TES are formulated analogously to BES.

Battery electric vehicle (BEV). In our case study we model multiple powered industrial trucks as special form of BEVs. BEVs are modeled as multiple energy storage systems $b \in \mathcal{B}$ similar to BESs but with restricted availability and two types of discharging: $\mathbf{P}_t^{\text{drive}}$ and $\mathbf{P}_t^{\text{V2X}}$. While $\mathbf{P}_t^{\text{drive}}$ is given exogenously through historic measurements, $\mathbf{P}_t^{\text{V2X}}$ can be activated ($z^{\text{V2X}}=1$) to allow V2X, i.e., smart discharging for non-driving purposes. Smart charging can be deactivated ($z^{\text{smart}}=0$) by penalizing the sum of charges weighted by the according time steps, see Eq. (28) and the objective function Eq. (2). Battery degradation was limited by constraining the minimum and maximum state of charge ($k_b^{\text{empty}}=0.15$, $k_b^{\text{full}}=0.85$) and the C rate ($\lambda_b^{\text{in}} = \lambda_b^{\text{out}} = 0.7$). Please see [56] for a recent review regarding battery degradation in DR scenarios. The BEV constraints are:

$$\mathbf{E}_{t,b} = \eta^{\text{time}} \begin{cases} k_b^{\text{ini}} \mathbf{E}_b^{\text{capn}} & \text{if } t = t_0 \\ \mathbf{E}_{t-1,b} & \text{otherwise} \end{cases} + \Delta t \left(\eta^{\text{ch}} \mathbf{P}_{t,b}^{\text{in}} - \frac{\mathbf{P}_{t,b}^{\text{drive}} + \mathbf{P}_{t,b}^{\text{V2X}}}{\eta^{\text{dis}}} \right) \quad \forall t \in \mathcal{T}, b \in \mathcal{B} \quad (23)$$

$$k_b^{\text{empty}} \mathbf{E}_b^{\text{capn}} \leq \mathbf{E}_{t,b} \leq k_b^{\text{full}} \mathbf{E}_b^{\text{capn}} \quad \forall t \in \mathcal{T}, b \in \mathcal{B} \quad (24)$$

$$\mathbf{P}_{t,b}^{\text{in}} \leq y_{t,b}^{\text{avail}} \lambda_b^{\text{in}} \mathbf{E}_b^{\text{capn}} \quad \forall t \in \mathcal{T}, b \in \mathcal{B} \quad (25)$$

$$\mathbf{P}_{t,b}^{\text{V2X}} \leq z^{\text{V2X}} y_{t,b}^{\text{avail}} \lambda_b^{\text{V2X}} \mathbf{E}_b^{\text{capn}} \quad \forall t \in \mathcal{T}, b \in \mathcal{B} \quad (26)$$

$$\mathbf{E}_{t_{\text{ref}},b} = k_b^{\text{ini}} \mathbf{E}_b^{\text{capn}} \quad \forall b \in \mathcal{B} \quad (27)$$

$$\mathbf{X}^{\text{penalty}} = (1 - z^{\text{smart}}) \sum_{t \in \mathcal{T}} \sum_{b \in \mathcal{B}} t \mathbf{P}_{t,b}^{\text{in}} \quad (28)$$

To reduce model complexity, we aggregated the capacity of 12 batteries that had similar availability patterns resulting in two batteries with 973.2 kWh capacity each and used two representative availability time series based on the real empirical data from the battery energy management system. Fig. 9 indicates the number of available batteries for charging across the year.

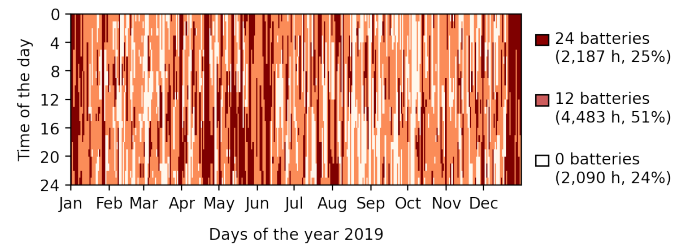


Fig. 9. Number of available batteries throughout the year 2019. The numbers and percentages in brackets indicate how often an availability appears. While all batteries are available in 2,187 hours (25% of the year), no battery is available in 2,090 hours (24%).

3.5. Limitations

The flexibility potentials of the applications spot market optimization, self-consumption optimization, and peak shaving in this paper are overestimated due to the following simplifications: (1) Perfect foresight is assumed for all input time series. (2) Battery degradation is limited by constraining the minimum and maximum state of charge but not explicitly modeled. (3) Batteries of powered industrial trucks are aggregated.

4. Evaluation metrics

4.1. Evaluation of DR based on prices and CEFs

Through penalizing or constraining operating CEs in a MES model considering price-based DR, CEFs can work as an additional DR incentive. E.g., if Scope I CEs are forced to be zero and Scope II CEs are penalized with a carbon price of $\text{€}222 \text{ t}_{\text{CO}_2\text{eq}}^{-1}$, the effective DR incentive is the sum of electricity prices and carbon price-weighted CEFs, presented in Fig. 10.

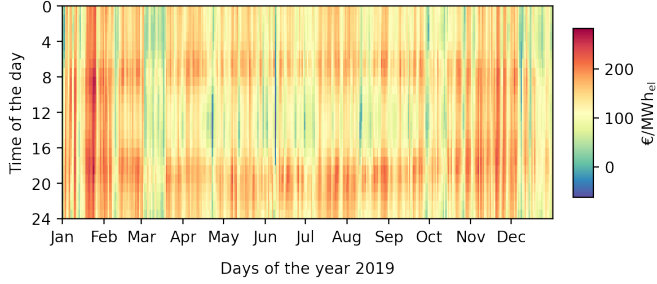


Fig. 10. Financial DR signal that consists of electricity prices of Fig. 7 plus the CEFs of Fig. 7 weighted by a carbon (removal) price of $222\text{€}/\text{t}_{\text{CO}_2\text{eq}}$.

To evaluate DR based on prices and CEFs, we define multiple related metrics. The energy-weighted average price (EWAP_s) and energy-weighted average CEF (EWACEF_s) are defined in Eqs. (29) and (30). For a scenario *s*, they measure the price and CEF of the average unit of purchased electricity respectively. While the EWAP is the total purchased electricity costs (excluding taxes and levies) divided by the total purchased electrical energy, the EWACEF is the quotient of the total CEs due to purchased electricity and the total purchased electrical energy. EWAP and EWACEF can be interpreted as the inability of the MES to react to the electricity prices and CEFs, respectively.

$$\underbrace{\text{EWAP}_s}_{\text{in } \text{€}/\text{MWh}} = \frac{\sum_{t \in \mathcal{T}} c_t^{\text{elec}} \mathbf{P}_{t,s}^{\text{EG,buy}} \Delta t}{\sum_{t \in \mathcal{T}} \mathbf{P}_{t,s}^{\text{EG,buy}} \Delta t} \quad (29)$$

$$\underbrace{\text{EWACEF}_s}_{\text{in } \text{t}_{\text{CO}_2\text{eq}}/\text{MWh}} = \frac{\sum_{t \in \mathcal{T}} \varepsilon_t^{\text{elec}} \mathbf{P}_{t,s}^{\text{EG,buy}} \Delta t}{\sum_{t \in \mathcal{T}} \mathbf{P}_{t,s}^{\text{EG,buy}} \Delta t} \quad (30)$$

For comparison, we define the time-weighted average price (TWAP) and the time-weighted average CEF (TWACEF):

$$\underbrace{\text{TWAP}}_{\text{in } \text{€}/\text{MWh}} = \frac{\sum_{t \in \mathcal{T}} c_t^{\text{elec}} \Delta t}{\sum_{t \in \mathcal{T}} \Delta t} \quad (31)$$

$$\underbrace{\text{TWACEF}}_{\text{in } \text{t}_{\text{CO}_2\text{eq}}/\text{MWh}} = \frac{\sum_{t \in \mathcal{T}} \varepsilon_t^{\text{elec}} \Delta t}{\sum_{t \in \mathcal{T}} \Delta t} \quad (32)$$

In simple terms, TWAP is the average price, EWAP is the average paid price, TWACEF is the average CEF, and EWACEF is the average accounted CEF. While TWAP and TWACEF only look at the electricity market results c_t^{elec} and $\varepsilon_t^{\text{elec}}$, EWAP and EWACEF also look at the profile of the demand-side electricity purchase $\mathbf{P}_t^{\text{EG,buy}}$.

Next, we define the π_s -rate and the ε_s -rate of scenario *s* by normalizing EWAP_s with TWAP and EWACEF_s with TWACEF:

$$\pi_s = \frac{\text{EWAP}_s}{\text{TWAP}} \quad (33)$$

$$\varepsilon_s = \frac{\text{EWACEF}_s}{\text{TWACEF}} \quad (34)$$

The π -rate has three advantages over EWAP. Firstly, it considers the price profile c_t^{elec} independently of the units, i.e., a European case study using € can be compared to an American using \$. Secondly, it is relative to the average price allowing comparison between time frames of different price levels, e.g., the years 2019 and 2021. Thirdly, it tells if the EWAP_s is over the TWAP ($\pi_s > 100\%$) or under ($\pi_s < 100\%$). The same advantages apply analogously to the ε -rate.

The time-based cost-emission ratio (TCER), is the scenario-independent ratio of the average electricity prices to the average CEF:

$$\underbrace{\text{TCER}}_{\text{in } \text{€}/\text{t}_{\text{CO}_2\text{eq}}} = \frac{\text{TWAP}}{\text{TWACEF}} \quad (35)$$

A TCER of $\text{€}100 \text{ t}_{\text{CO}_2\text{eq}}^{-1}$, e.g., means that if a load is reduced equally over all time steps, €100 is saved for each reduced ton of CEs. On an energy-specific price-emission diagram with flexibility metrics Fig. 11, TCER is the gradient of the line between the origin and the intersection between the TWAP and the TWACEF.

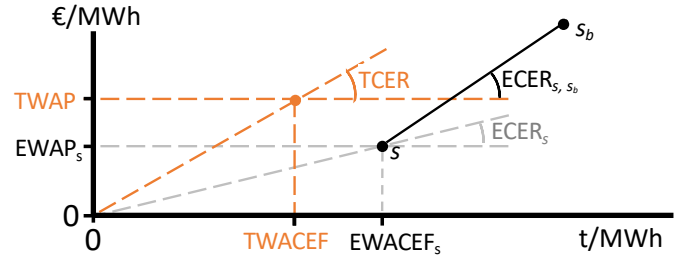


Fig. 11. Energy-specific price-emission diagram to illustrate flexibility metrics.

In contrast, the energy-based cost-emission ratio (ECER) of scenario *s* is the ratio of EWAP_s to EWACEF_s:

$$\underbrace{\text{ECER}_s}_{\text{in } \text{€}/\text{t}_{\text{CO}_2\text{eq}}} = \frac{\text{EWAP}_s}{\text{EWACEF}_s} \quad (36)$$

On an EWAP-EWACEF plot, the ECER_s is the gradient of the line between the origin and the scenario *s*, see Fig. 11.

Next, we define the ECER for two scenarios, *s* and *s_b*, where *s_b* is the baseline scenario without flexibility:

$$\underbrace{\text{ECER}_{s,s_b}}_{\text{in } \text{€}/\text{t}_{\text{CO}_2\text{eq}}} = \frac{\text{EWAP}_{s_b} - \text{EWAP}_s}{\text{EWACEF}_{s_b} - \text{EWACEF}_s} \quad (37)$$

ECER_{s,s_b} can be also interpreted as the ratio of electrical energy cost savings to CE savings of scenario *s* compared to the baseline scenario *s_b*. E.g., an ECER_{a,b} of $\text{€}150 \text{ t}_{\text{CO}_2\text{eq}}^{-1}$ means that on

average €150 is saved for each reduced ton of CEs. On the EWAP-EWACEF plot, $ECER_{s,s_b}$ represents the gradient of the line between s and s_b , see Fig. 11. When assessing DR, i.e., the modification of $P_f^{EG,buy}$, $ECER_{s,s_b}$ can be interpreted as how strongly cost reduction is weighted relative to CE reduction.

Finally, based on the previous metrics, we define the normalized gradients ω_s and ω_{s,s_b} :

$$\omega_s = \frac{\pi_s}{\varepsilon_s} = \frac{ECER_s}{TCER} \quad (38)$$

$$\omega_{s,s_b} = \frac{\pi_s - \pi_{s_b}}{\varepsilon_s - \varepsilon_{s_b}} \quad (39)$$

They have the same advantages over $ECER_s$ then the π -rate has over EWAP.

The metrics defined in Section 4.1 can be applied to any price and load data set. Also, they can be applied to a subset of data, e.g., months or weekdays. It is worth mentioning that while the EG feed-in also impacts the stability of the EG and the electricity markets, the evaluation of EG feed-in is beyond the scope of this paper.

4.2. Evaluation of decarbonization costs

To evaluate the additional cost of achieving net-zero CEs, we calculate the decarbonization costs C_s^{decarb} :

$$C_s^{decarb} = TAC_{s_d} - TAC_s \quad (40)$$

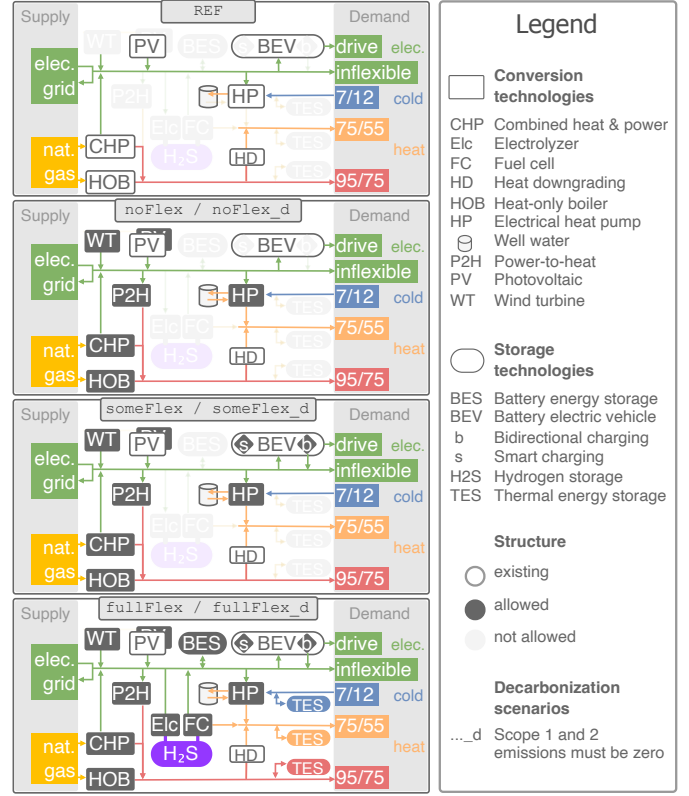
where the scenarios s_d and s represent the cost optimal MES with and without enforcing net-zero CEs, respectively.

5. Scenario and context definition

5.1. Scenario definition

We model seven scenarios: One unoptimized reference scenario (REF), three optimized non-decarbonization scenarios (noFlex, someFlex, fullFlex), and three optimized decarbonization scenarios (noFlex_d, someFlex_d, fullFlex_d). The scenario definition is summarized in Fig. 12 and described in the following:

- REF: The reference scenario represents the unoptimized status quo, also described in Fig. 4. Electricity demand is covered by the EG, the PV, and the CHP. BEVs are charged unidirectionally with full power until full. Heat demands are met by the CHP and the HOB. The cold demand is served by the cooling machine which was modeled as a HP with 1,147 kW on the hot side and in a restricted mode so that heat in the condenser is only transferred to the well water. We assume that the cooling machine only exists in the REF scenario and must be replaced in other scenarios, to make the results comparable between them. There are no energy storage systems. Investments are deactivated.
- noFlex: Investments in the conversion technologies WT, PV, HP, P2H are allowed. According capacities are optimally designed. The smart HP mode selection is deactivated by disallowing heat transfer from cold to heat demand. Fuel switching is deactivated by fixing the CHP operation to the CHP operation in REF. Smart/bidirectional



↓ Possible options	Scenarios →	noFlex,	someFlex,	fullFlex,
	REF	noFlex_d	someFlex_d	fullFlex_d
Conversion tech. investments ^a	x	✓	✓	✓
Use of existing flexibility ^b	x	x	✓	✓
Storage tech. investments ^c	x	x	x	✓

^a WT, PV, HP, and P2H

^b smart/bidirectional BEV charging, fuel switching, and smart HP mode selection

^c BES, TES (on all temperature levels), and H₂S (including Elc and FC)

Fig. 12. Definition of scenarios

BEV charging and investments in storage systems are deactivated.

- someFlex: Additionally to noFlex, some flexibility sources can be used: BEVs can be charged smartly/bidirectionally. For each time step heat supply can be chosen to be gas-based (HOB, CHP) and/or electricity-based (HP, P2H), since the restriction to the CHP operation is removed. However, storage investments are still deactivated.
- fullFlex: Additionally, investments in the following storage technologies are allowed: BES, TES (on all three temperature levels), and H₂S including Elc and FC with waste heat utilization on the 75/55 temperature level.
- noFlex_d, someFlex_d, fullFlex_d: Decarbonization scenarios based on noFlex, someFlex, and fullFlex, respectively. Scope 1 and 2 carbon neutrality is enforced. Natural gas is strictly forbidden to prevent investments in and operation of fossil-based infrastructure. Electricity-based CEs must be removed with the specific carbon removal costs c^{DAC} .

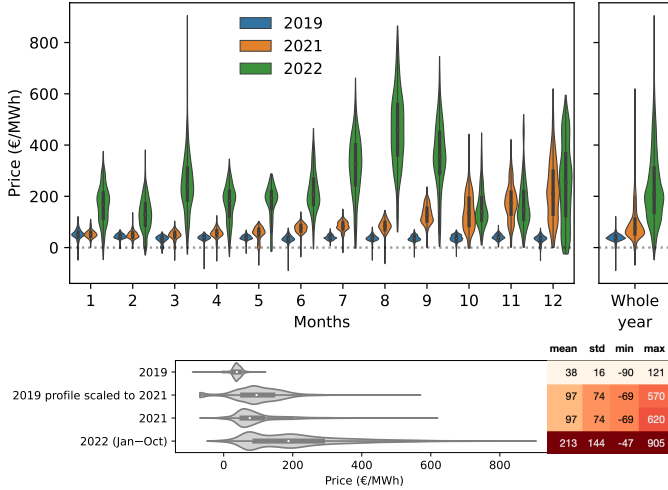


Fig. 13. Distribution of day-ahead electricity market prices of 2019, 2021, and 2022 (top, until October) and the used 2019 profile that was scaled to 2021 levels (bottom).

Table 2
Definition of contexts

Context	Carbon removal price c^{DAC}	Electricity price c_t^{elec}
c_base	$\text{€}222 \text{ t}_{\text{CO}_2\text{eq}}^{-1}$	2019 data
c_strict	$\text{€}10.000 \text{ t}_{\text{CO}_2\text{eq}}^{-1}$	2019 data
c_scaled	$\text{€}222 \text{ t}_{\text{CO}_2\text{eq}}^{-1}$	2019 data scaled to 2021

5.2. Context definition

We model all scenarios for the three contexts defined in Table 2. c_base is the base context with electricity price data of 2019 and specific carbon removal costs c^{DAC} of $\text{€}222 \text{ t}_{\text{CO}_2\text{eq}}^{-1}$ – the specific costs of direct air capturing [57]. In c_strict, electricity price data of 2019 is used but c^{DAC} is set to $\text{€}10 \text{ k t}_{\text{CO}_2\text{eq}}^{-1}$. If this high price is paid, the onsite decarbonization is not viable. This context applies when a company does not plan to rely on carbon removal or on the carbon reductions of the electricity grid. In c_scaled, c^{DAC} is $\text{€}222 \text{ t}_{\text{CO}_2\text{eq}}^{-1}$ but the electricity prices are scaled to 2021 levels. By picking the year 2019 as base year, the quantified value of flexibility is underestimated due to the relatively low price spreads on the day-ahead market, see Fig. 3, however, energy demands don't feature anomalies from the COVID-19 crisis. Therefore, in c_scaled, we scaled the day-ahead market prices of the year 2019 to roughly match the mean, the standard deviation, and the extreme points of the prices of 2021, see Fig. 13. All other time series such as energy demands, vRES profiles, and electricity grid CEFs are kept unchanged. By avoiding the combination of time series from different years, correlations between day-ahead market prices, thermal loads, and renewable energy generation are maintained. Also we do not use the 2022 price distribution since we assume that they are overestimating the potential due to short-term consequences of the Russian invasion of Ukraine.

6. Results

In this section, the results of the three contexts are described sequentially and discussed at the end. The MILP models were solved to global optimality (MIP gap=0) using Gurobi 9.5.1. The calculation time for one optimization run with seven scenarios was between 10 and 80 minutes depending on the context. The discount rate r was assumed to be 10% for all calculations.

6.1. Results of the base context c_base

Figs. 14 to 18 and A.22 to A.26 and Table 3 show the results of the base context c_base.

The Sankey plots in Fig. A.26 provide an overview of the resulting annual energy sums of the MES for each scenario. It can be seen that the heat demands were partly electrified in the non-decarbonization scenarios and fully electrified in the decarbonization scenarios.

Table 3
New capacities for the c_base context

	PV (kW _p)	WT (kW _P)	HP (kW _{th,cond})	P2H (kW _{th})	TES (kWh _{th})
noFlex	1,356	0	918	105	0
someFlex	2,853	0	907	197	0
fullFlex	3,028	0	760	222	3,216
noFlex_d	3,077	2,183	1,723	485	0
someFlex_d	3,077	2,140	1,049	863	0
fullFlex_d	3,077	2,344	899	1,082	14,675

Table 3 shows the resulting new capacities. Additional PV capacity was installed in all non-REF scenarios. In contrast to the decarbonization scenarios, in the non-decarbonization scenarios the upper limit of 3,077 kW_p was not chosen. WTs were only selected in the decarbonization scenarios ranging from 2,140 kW_p to 2,344 kW_p. HPs were built in all non-REF scenarios ranging from 760 kW_{th} in fullFlex to 1,723 kW_{th} in noFlex_d. P2Hs were built in all non-REF scenarios increasing from 105 kW_{th} in noFlex to 1,082 kW_{th} in fullFlex_d. TESs were optimal in fullFlex (3,216 kWh_{th}) and fullFlex_d (14,675 kWh_{th}). Whereas in fullFlex, the largest TES was built on the cooling temperature level, in fullFlex_d the largest was built on the process heat temperature level. No BES or H₂S was selected.

Fig. 18 displays the annual balances for costs, CEs, peak power, and energy streams and of all scenarios and its deviations compared to noFlex and noFlex_d, respectively. It can be seen in a) and b) that adding flexibility reduces TACs and CEs. someFlex has 10.4% less TACs and 17.1% less CEs than noFlex. fullFlex has 11.7% less TACs and 20.1% less CEs than noFlex. In the decarbonization case (..._d), the TAC reductions were even more pronounced. someFlex_d has 6.5% and fullFlex_d 15.0% less TACs than noFlex_d. c) and d) show that someFlex has 67.4% higher CapEx but 19% lower OpEx than noFlex. Similarly, someFlex_d has 78% higher CapEx but 21.8% lower OpEx than noFlex. Interestingly, someFlex_d has both lower CapEx and OpEx while fullFlex_d has 6.5% higher CapEx and 26.7% lower OpEx than noFlex_d. From e) and f), we can see that while the purchased electricity $W^{\text{EG,buy}}$ were comparable for all scenarios, the

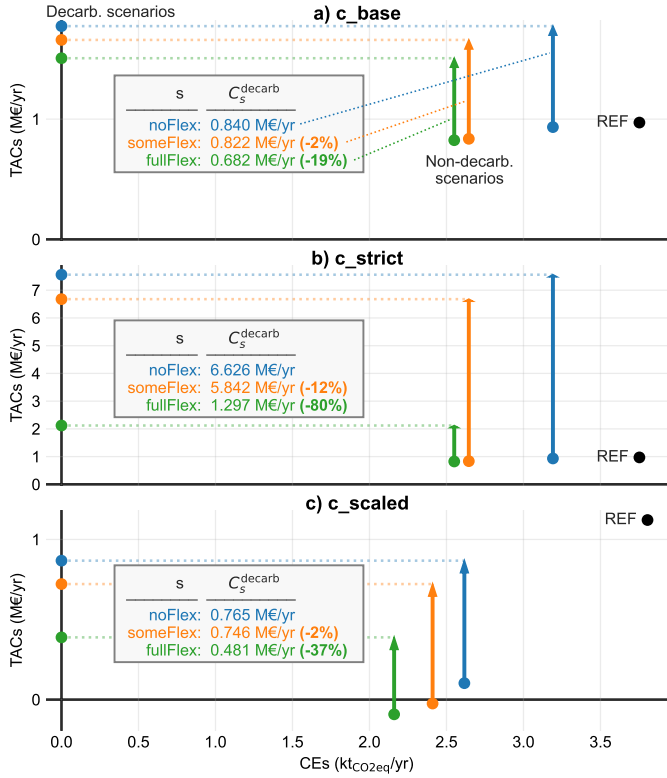


Fig. 14. Pareto plots and decarbonization costs C_s^{decarb} for the three contexts. Note, the results of the non-decarbonization scenarios for c_{base} and c_{strict} are identical. Percentages are based on noFlex.

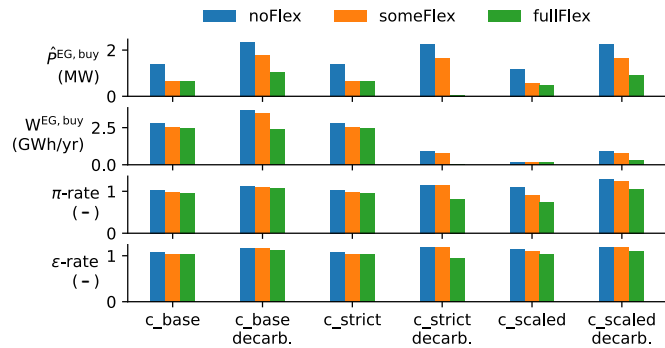


Fig. 15. Comparison of $\hat{p}^{\text{EG},\text{buy}}$, $W^{\text{EG},\text{buy}}$, π -rate, and ϵ -rate of all optimized scenarios of all contexts. Here, decarb. denote the decarbonization scenarios noFlex_d, someFlex_d, and fullFlex_d.

electricity purchase peak $\hat{p}^{\text{EG},\text{buy}}$ in someFlex and fullFlex were reduced by over 50% compared to noFlex and in some Flex_d and fullFlex_d by 24.2% and 54.9% reduced compared to noFlex_d, respectively. From g) we see that while in REF, as expected, the HP was only used in cooling mode, in the noFlex scenarios, the HP was also used for heating. In someFlex and someFlex_d already most of the cooling energy being used for heating and going to the fullFlex scenarios, this share was increased, so only a small fraction of the cooling energy is lost to well water.

Fig. A.25 indicates the electricity balance of one week in May for all scenarios of c_{base} and the day-ahead electricity

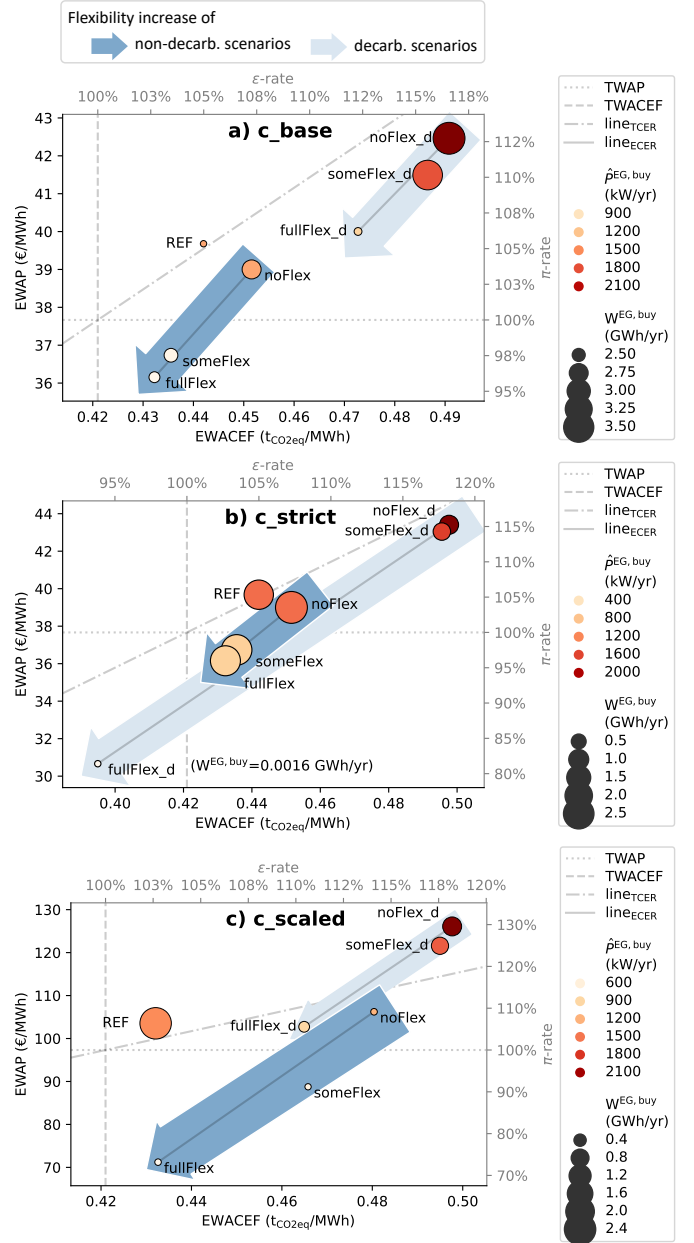


Fig. 16. Bubble plot of EWAP and EWACEF of purchased electricity for the three contexts. Dark blue and light blue arrows indicate the flexibility increase of non-decarbonization and decarbonization scenarios, respectively. Solid grey lines inside the arrows connect noFlex and fullFlex and have the gradient $\text{ECER}_{\text{fullFlex}_d, \text{noFlex}_d}$. Dotted and dashed lines indicate the context-independent TWAP and TWACEF, respectively. Bubble color correspond to electricity peak purchase power $\hat{p}^{\text{EG},\text{buy}}$. Bubble size represents the total electricity purchase volume $W^{\text{EG},\text{buy}}$. Note, the results of the non-decarbonization scenarios for c_{base} and c_{strict} are identical.

price c_t^{elec} . In someFlex and fullFlex, fuel switches from natural gas (CHP) to electricity (P2H) are observable during times of high PV supply. In all scenarios with flexibility, V2X activity can be seen in times of low PV and WT energy supply and/or high electricity prices. High activities of flexible loads (HP, P2H, BEV) can be seen in times of high PV and WT energy supply and/or low electricity prices. In fullFlex_d, own renewable energy is almost entirely used and not fed-in. By comparing

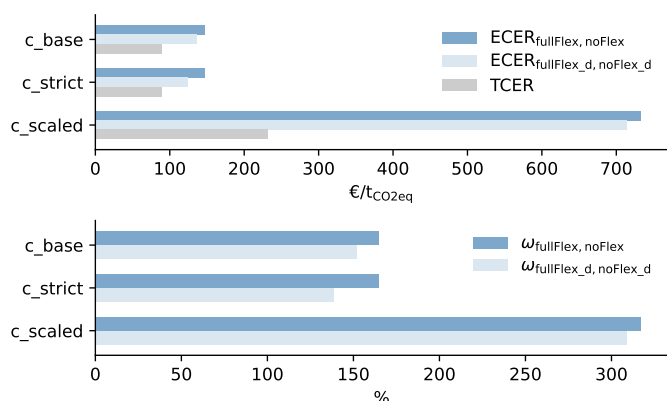


Fig. 17. Comparison of the gradients of the lines in Fig. 16. Top: Absolute gradients (in €/tCO_{2eq}) with TCER as comparison (i.e., gradient of line_{TCER} in Fig. 16). Bottom: Gradients relative to TCER (in %).

fullFlex with noFlex, it can be seen how the EG purchase profile is shaved.

Fig. A.23 presents the number of full V2X discharges per year. Interestingly, the fullFlex scenarios feature less discharges than the someFlex scenarios.

Fig. 14 a) depicts the pareto plot and the decarbonization costs C_s^{decarb} for the c_base context. It can be seen that C_s^{decarb} were 2% and C_s^{decarb} 19% lower than C_s^{decarb} noFlex.

The added flexibility is also used for price-based and CEF-based DR, i.e., to optimize the electricity purchase against electricity prices and CEFs, respectively. The EWAP and EWACEF are good indicators for this. They are shown in Fig. 16 a) for all scenarios together with the annual sum and the peak of the electricity purchase. It can be seen that with increasing flexibility, electricity purchase decreases in volume ($W^{\text{EG, buy}}$), peak ($\hat{p}^{\text{EG, buy}}$), carbon intensity (EWACEF), and price (EWAP). In other words, the flexibility allows for greener and cheaper purchases of less electricity. It can also be seen that the dark blue arrow (indicating non-decarbonization scenarios) crosses the TWAP line since in someFlex and fullFlex, the EWAP is lower than the TWAP while in noFlex, the EWAP is higher than the TWAP. This shows that flexibility reduced the average paid price (EWAP) to below the average price (TWAP).

Fig. 17 shows the gradients of line_{TCER} and line_{ECER} in Fig. 16. As expected, the gradient in the decarbonization case is lower than in the non-decarbonization case.

6.2. Results of the strict decarbonization context c_strict

The results of the c_strict context are shown in Figs. 14 to 17, 19, 20, A.22, A.24 and A.27 and Table A.4. In c_strict, C_s^{decarb} were 12% and C_s^{decarb} 80% lower than C_s^{decarb} noFlex, see Fig. 14 b). Even with a carbon removal price of $\text{€}10\text{k t}^{-1}\text{CO}_{2\text{eq}}$ in noFlex_d and someFlex_d significant amounts of electricity-based CEs were removed to reach carbon neutrality, while in fullFlex_d carbon removal was not necessary, see Fig. 20 b). This demonstrates that strict decarbonization without energy flexibility is infeasible, at least when the 2019 power plant mix is assumed. In fullFlex_d, strict decarbonization was possible without carbon removal by investing in BES, TES, and H₂S

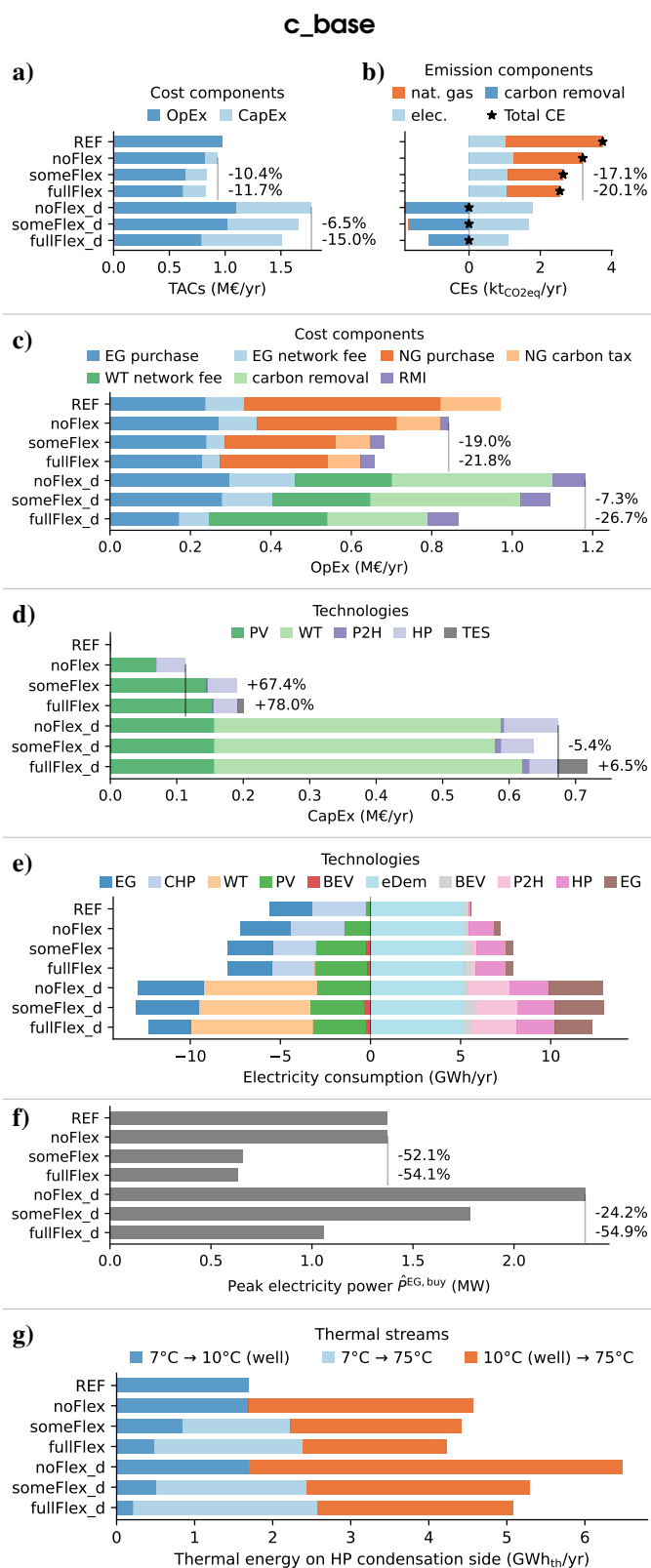


Fig. 18. Annual results of the c_base context. **a)** Total annualized costs (TACs), **b)** operating carbon emissions (CEs), **c)** operating expenses (OpEx), **d)** capital expenditures (CapEx), **e)** electricity consumption (+) and supply (-), **f)** electricity purchase peaks, **g)** heat pump (HP) operation. **Note:** Percentages refer to noFlex or noFlex_d.

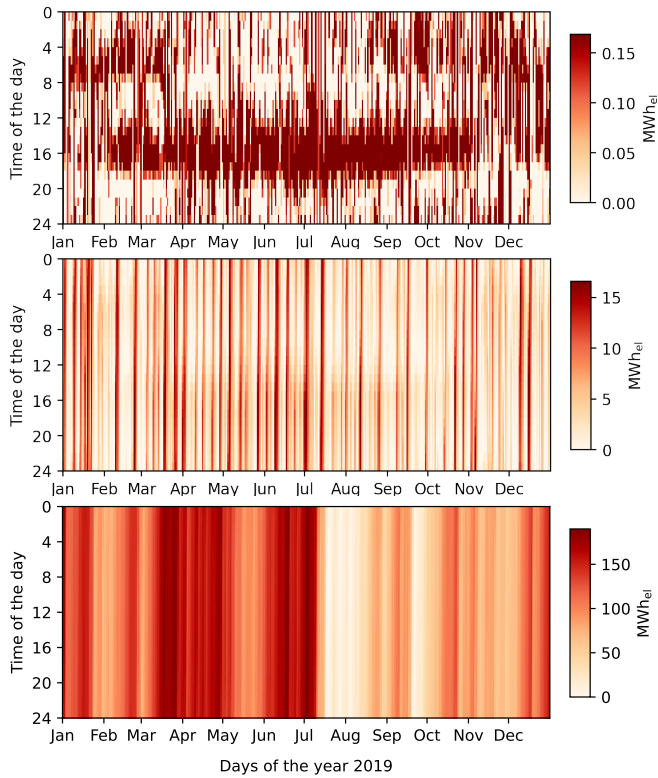


Fig. 19. Energy filling level of BES (top), 97/75-TES (middle), and H₂S (bottom) in scenario fullFlex_d of context c_strict.

technologies, see Fig. A.27, Fig. 20 b), and Table A.4. While the BES stored (mainly solar) energy for a few hours, the TES stored energy for a few days, and the H₂S stored energy for multiple days or weeks, see Fig. 19. The reason for this is that H₂ storage chains (Elc, H₂S, FC) feature higher kW-costs and lower kWh-costs than BESs. By comparing Fig. 19 bottom and Fig. 8, it can be seen that the H₂S is completely discharged to cover several days of low solar and wind generation in the mid of July. Through storage technologies (BES, TES, H₂S) the WT capacity of noFlex_d and someFlex_d can be reduced from over 19 MW_p to 5.3 MW_p, see Table A.4.

The long blue arrow in Fig. 16 b) indicates a wide range of EWAP and EWACEF for the decarbonization scenarios. Whereas in noFlex_d and someFlex_d, the metrics (EWAP, EWACEF, $\hat{P}^{EG, buy}$, and $W^{EG, buy}$) differed only slightly compared to c_base, in fullFlex_d, they were very low compared to the other scenarios. This reveals that in fullFlex_d, the flexibility was not only used to optimize self-consumption and buy less electricity but also to buy in hours of lower prices and CEFs.

The fullFlex_d scenario features 71.9% less TACs than noFlex_d. What is striking is that through the flexibility, the CapEx could be lowered by 54.6% mainly due to less WT capacity and the OpEx could be lowered by 86.5% mainly due to avoiding carbon removal costs.

6.3. Results of the scaled electricity price context c_scaled

The results of the c_scaled context are shown in Figs. 14 to 17, 21, A.22, A.24 and A.28 and Table A.4. In c_scaled,

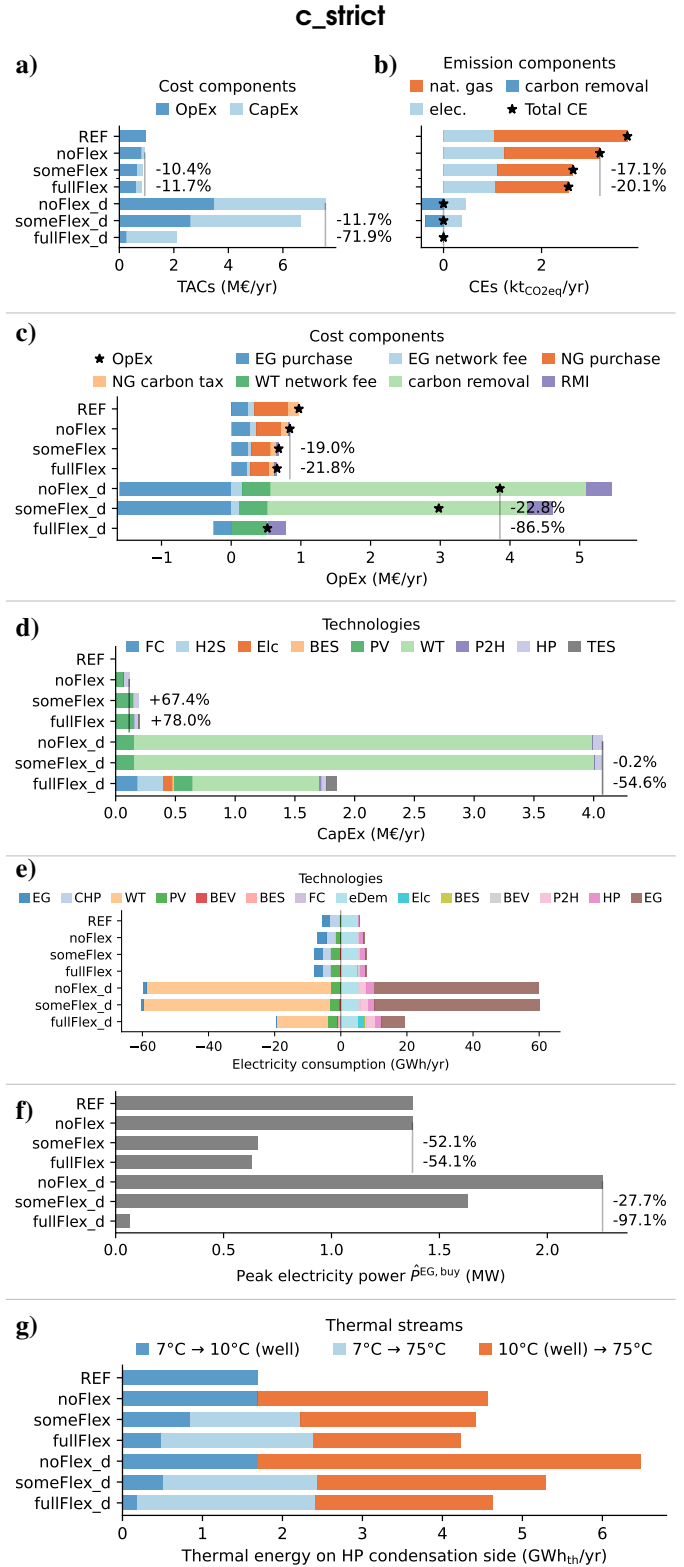


Fig. 20. Annual results of the c_strict context. a) Total annualized costs (TAC), b) operating carbon emissions (CEs), c) operating expenses (OpEx), d) capital expenditures (CapEx), e) electricity consumption (+) and supply (-), f) electricity purchase peaks, g) heat pump (HP) operation. **Note:** Percentages refer to noFlex or noFlex_d.

$C_{\text{someFlex}}^{\text{decarb}}$ were 2% and $C_{\text{fullFlex}}^{\text{decarb}}$ 37% lower than $C_{\text{noFlex}}^{\text{decarb}}$, see Fig. 14 c). In contrast to c_{base} , in c_{scaled} a (small) BES was selected in fullFlex and the maximum possible PV capacity of 3.077 MW_p was chosen in the non-decarbonization scenarios (noFlex, someFlex, and fullFlex), see Table A.4. TACs of the non-decarbonization scenarios were significantly reduced compared to the other contexts, showing even negative TAC values for someFlex and fullFlex, see Fig. 14 c). I.e., assuming the level and fluctuation of the electricity prices of the year 2021, the company's MES (together with offshore WTs) can be seen as a business model with an above 10% internal return rate, provided that the WT installation is feasible. However, WT capacity is limited by the maximum feed-in of 20 MWh/h, which can be seen in Fig. A.22. As a result, WT capacities of 19–22 MW_p were selected (see Table A.4) even though most of it was sold on the day-ahead market. Fig. 16 c) shows that adding flexibility reduced EWAP, EWACEF, $\hat{P}^{\text{EG, buy}}$, and $W^{\text{EG, buy}}$. Due to the high WT capacities, the level of $W^{\text{EG, buy}}$ for all optimized scenarios was low compared to REF. From Fig. 17 we can see that, for c_{scaled} , both ω values are over 300%, i.e., in the decarbonization and non-decarbonization case, ECER were more than three times the TCER, or in other words, the modification of $P_t^{\text{EG, buy}}$ in c_{scaled} proportionately reduced significantly more costs than CEs.

6.4. Discussion of the results

When comparing all scenarios and contexts, the following results are striking:

1. In all analyzed contexts, adding flexibility significantly reduced TACs and CEs. TAC reductions were between 10.4 and 189.6%. However, the high reduction of 189.6% was based on the already very low TAC of €0.10M/yr in the c_{scaled} noFlex scenario. The second-highest relative TAC decrease appeared in the decarbonization case of c_{strict} with 71.9%. This was because c_{strict} fullFlex_d was the only scenario reaching carbon neutrality without carbon removal since flexibility increased the self-consumption which eliminated the need for expensive carbon removal. While the someFlex scenarios showed 7.9–17.1% CE reductions compared to noFlex, the fullFlex scenarios showed 17.1–20.1%.
2. Through storage investments and the smart/bidirectional charging of existing powered industrial trucks (fullFlex), decarbonization costs decreased by 19% in c_{base} (assuming $c^{\text{DAC}} = \text{€}222 \text{ t}_{\text{CO}_2\text{eq}}^{-1}$ and 2019 electricity prices). This number increased to 37% in c_{scaled} (assuming $c^{\text{DAC}} = \text{€}222 \text{ t}_{\text{CO}_2\text{eq}}^{-1}$ and 2019 electricity prices scaled to 2021 levels), and further increased to 80% in c_{strict} (assuming $c^{\text{DAC}} = \text{€}10 \text{ k t}_{\text{CO}_2\text{eq}}^{-1}$ and 2019 electricity prices).
3. With current CEFs, the MES could technically only achieve strict Scope I and II net-zero CEs (c_{strict}) when using the full flexibility potential (fullFlex_d) of different mutually complementary energy storage technologies, one of them being H₂S which aligns with the results of Petkov and Gabrielli [28]. However, due to the high CapEx, it seems rather unrealistic, even if the full flexibility potential is considered. In contrast, if assuming electricity

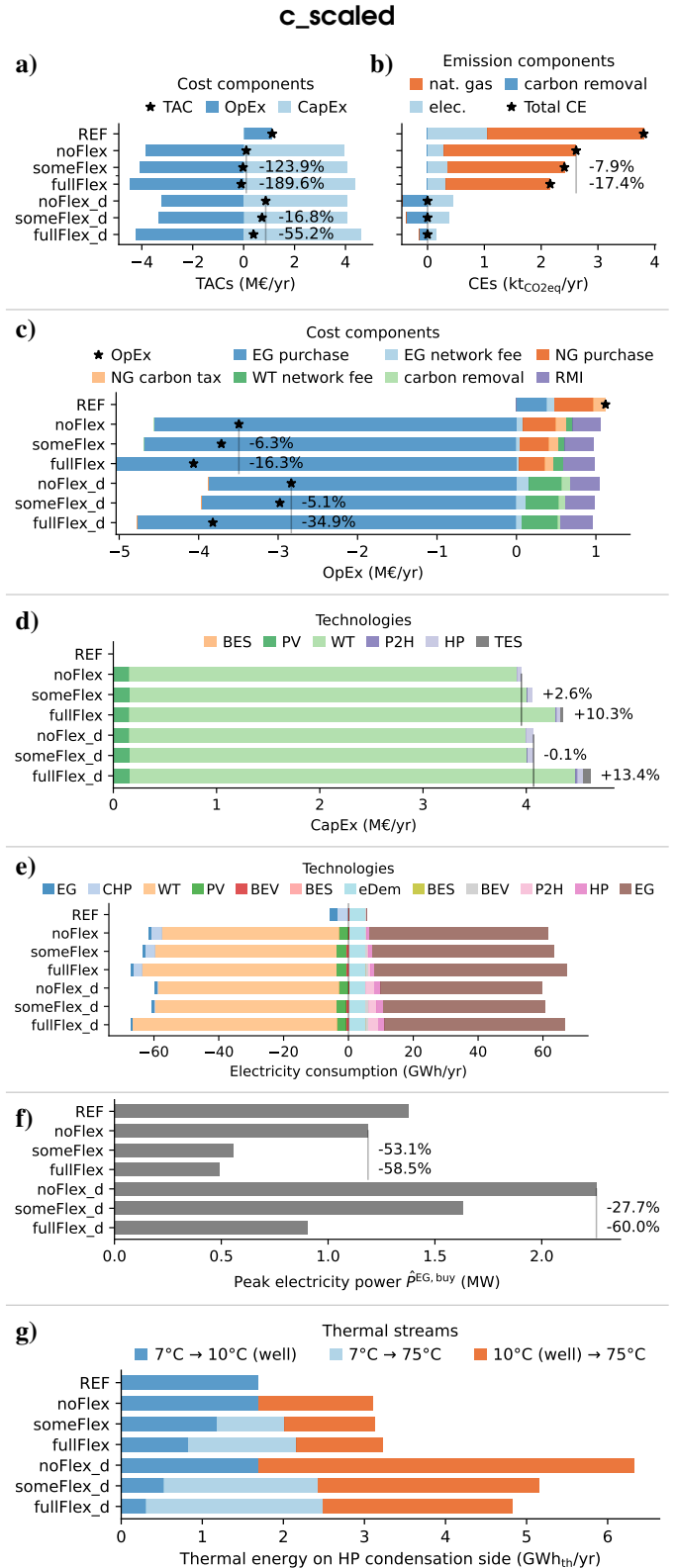


Fig. 21. Annual results of the c_{scaled} context. **a)** Total annualized costs (TAC), **b)** operating carbon emissions (CEs), **c)** operating expenses (OpEx), **d)** capital expenditures (CapEx), **e)** electricity consumption (+) and supply (-), **f)** electricity purchase peaks, **g)** heat pump (HP) operation. **Note:** Percentages refer to noFlex or noFlex_d.

grid decarbonization, which we indirectly did in c_base and c_scaled with a considerable price of $\text{€}222 t_{CO_2eq}^{-1}$ on electricity-based CEs, full decarbonization is realistic, especially when considering the full flexibility potential. When comparing $fullFlex_d$ to REF, TACs increased by 55% in c_base and decreased by 65% in c_scaled . However, the economic benefits of c_scaled mainly stem from wind power feed-in, see Fig. A.22. In any circumstance, the results showed that both the existing and the added flexibility through storage and sector coupling is highly valuable especially for the decarbonization and can be used for multiple purposes including price and CEF-based DR, peak shaving, and self-consumption optimization.

4. In all cases, $\hat{P}^{EG, buy}$, $W^{EG, buy}$, π -rate, and ε -rate reduced with increasing flexibility (see Fig. 15), i.e., price and CEF-based DR is used together with peak shaving and self-consumption optimization. All scenarios except the c_strict $fullFlex_d$ feature an ε -rate above 100%, i.e., the average accounted CEF (i.e., EWACEF) was above the average CEF (i.e., TWACEF). In the case of REF, the reason for this was the high electrical and thermal energy demand at business hours, where CEFs tend to be above average. REF and $noFlex_d$ of all contexts featured π and ε -rates of above 100%, i.e., without flexibility use, their electricity purchase profiles are less market-serving than a flat load profile. All dark blue arrows in Fig. 16 crossed the TWAP line from above, i.e., by using flexibility in the non-decarbonization case, the π -rate declined from above 100% to below 100%, or, put differently, the average paid price (i.e., EWAP) fell below the average price (i.e., TWAP).
5. The results in Fig. 16 show that the DR evaluation metrics proposed in Section 4.1 are simple, tangible and useful to compare and visualize the intensity of price and CEF-based DR in a meaningful way. The metrics EWAP and EWACEF are especially tangible since they have the same unit as the prices and CEFs, and can be compared to the TWAP and TWACEF, respectively. The metrics π -rate and ε -rate stand out when comparing scenarios under different contexts. Due to the normalization with TWAP and TWACEF, they are independent from the level of prices and CEFs, respectively. However, when evaluating price-based and CEF-based DR, $\hat{P}^{EG, buy}$ and $W^{EG, buy}$ should also be considered to account for interactions with peak shaving and self-consumption optimization. The metrics TCER and ECER measure the dominance of prices versus CEFs as signal for DR and can be interpreted as gradients in a price-CEF diagram.
6. As expected, the results of c_scaled demonstrate that high and highly fluctuating electricity prices incentivize the activation of existing flexibility as well as investments in vRES and energy storage systems. E.g., while the V2X activity was similar in c_base and c_strict , it was up to 2.7x higher in c_scaled with 498 full V2X discharges per year (=1.36 per day) in $someFlex_d$, see Fig. A.23. Since energy shock scenarios, like in the year 2022, might

not be a once-in-a-century event in a time of political instability, it might be interesting to quantify the value of being a flexumer in such a price shock scenario.

7. Conclusions

This study quantified the value of flexibility for decarbonizing a production company's MES within a detailed optimal design and operation case study considering and evaluating price-based and CEF-based DR. Based on the case study results discussed in Section 6.4, the following conclusions can be drawn:

- Production companies can significantly reduce TACs, CEs, and decarbonization costs by using the energy flexibility of their MES (Items 1 and 2).
- A strict net-zero CE MES is only achieved using energy flexibility. To achieve net-zero CEs in a cost-effective manner, comparative advantages of energy storage systems are used (Item 3).
- Independently from electricity prices and decarbonization ambitions, less, greener, and cheaper electricity is purchased when using energy flexibility (Item 4).
- The flexibility metrics defined in Section 4.1 are simple, tangible, and effective to evaluate the intensity of DR based on prices and CEFs (Item 5).
- High electricity prices encourage vRES investments and are, due to market mechanisms, typically accompanied by increased price volatility which incentivizes operational flexibility through energy storage investments and price-based DR (Item 6).

The findings of this study underline the significant potential of energy flexibility to reduce costs, CEs, and fossil fuel dependency for manufacturing companies. They illustrate the importance of considering future electricity price fluctuations, decarbonization goals, and the company's assessment of future carbon removal within the planning of sustainable MESs. Also, they demonstrate the multifaceted techno-economic interactions of modern sustainable MESs and, therefore, highlight the importance of integrated models for planning and flexibility potential evaluation.

Acknowledgments

This research was performed as part of the MeSSO Research Group at the Munster Technological University (MTU) and in relation to the project WIN4climate as part of the National Climate Initiative financed by the Federal Ministry for Economic Affairs and Climate Action (BMWK) on the basis of a decision by the German Bundestag (No. 03KF0094A). It was additionally funded by the MTU Risam scholarship scheme.

Declaration of competing interest

The authors declare that they have no known competing financial interests or personal relationships that could have appeared to influence the work reported in this paper.

CRedit authorship contribution statement

Markus Fleschutz: Conceptualization, Methodology, Software, Validation, Formal analysis, Investigation, Data Curation, Writing - original draft, Writing - review & editing, Visualization. **Markus Bohlayer:** Methodology, Writing - review & editing. **Marco Braun:** Supervision, Project administration, Funding acquisition. **Michael D. Murphy:** Supervision, Conceptualization, Writing - review & editing, Funding acquisition.

References

- [1] European Commission, *A European Green Deal* (2020). URL https://ec.europa.eu/info/strategy/priorities-2019-2024/european-green-deal_en
- [2] United Nations Environment Programme, *Emissions gap report 2021: The heat is on – a world of climate promises not yet delivered* (2021-10). URL <https://wedocs.unep.org/20.500.11822/36990>
- [3] A. W. Mortensen, B. V. Mathiesen, A. B. Hansen, S. L. Pedersen, R. D. Grandal, H. Wenzel, The role of electrification and hydrogen in breaking the biomass bottleneck of the renewable energy system – A study on the Danish energy system. *Applied Energy* 275 (2020) 115331. doi:10.1016/j.apenergy.2020.115331.
- [4] J. Rissman, C. Bataille, E. Masanet, N. Aden, W. R. Morrow, N. Zhou, N. Elliott, R. Dell, N. Heeren, B. Huckestein, J. Cresko, S. A. Miller, J. Roy, P. Fennell, B. Cremmins, T. Koch Blank, D. Hone, E. D. Williams, S. de La Rue Can, B. Sisson, M. Williams, J. Katzenberger, D. Burtraw, G. Sethi, H. Ping, D. Danielson, H. Lu, T. Lorber, J. Dinkel, J. Helseth, Technologies and policies to decarbonize global industry: Review and assessment of mitigation drivers through 2070, *Applied Energy* 266 (2020) 114848. doi:10.1016/j.apenergy.2020.114848.
- [5] F. Knobloch, S. Hanssen, A. Lam, H. Pollitt, P. Salas, U. Chewprecha, M. A. J. Huijbregts, J.-F. Mercure, Net emission reductions from electric cars and heat pumps in 59 world regions over time, *Nature sustainability* 3 (6) (2020) 437–447. doi:10.1038/s41893-020-0488-7.
- [6] A. Arteconi, D. Patteeuw, K. Bruninx, E. Delarue, W. D’haeseleer, L. Helsen, Active demand response with electric heating systems: Impact of market penetration, *Applied Energy* 177 (2016) 636–648. doi:10.1016/j.apenergy.2016.05.146.
- [7] IEA, *World energy outlook 2021* (2021). URL <https://www.iea.org/reports/world-energy-outlook-2021>
- [8] P. Mancarella, MES (multi-energy systems): An overview of concepts and evaluation models, *Energy* 65 (2014) 1–17. doi:10.1016/j.energy.2013.10.041.
- [9] D. Papadaskalopoulos, R. Moreira, G. Strbac, D. Pudjianto, P. Djapic, F. Teng, M. Papapetrou, Quantifying the Potential Economic Benefits of Flexible Industrial Demand in the European Power System, *IEEE Transactions on Industrial Informatics* 14 (11) (2018) 5123–5132. doi:10.1109/TII.2018.2811734.
- [10] Y. Jee, E. Lee, K. Baek, W. Ko, J. Kim, Data-Analytic Assessment for Flexusers Under Demand Diversification in a Power System, *IEEE Access* 10 (2022) 33313–33319. doi:10.1109/ACCESS.2022.3162077.
- [11] ENTSO-E, *ENTSO-E Transparency Platform* (2022). URL <https://transparency.entsoe.eu>
- [12] J. Mays, Missing incentives for flexibility in wholesale electricity markets, *Energy Policy* 149 (November 2020) (2021) 112010. doi:10.1016/j.enpol.2020.112010.
- [13] P. P. Raimondi, *Natural gas pricing mechanisms and the current crisis: drivers and trends*. URL <https://perma.cc/3KL9-YGNF>
- [14] F. Sensfuß, M. Ragwitz, M. Genoese, The merit-order effect: A detailed analysis of the price effect of renewable electricity generation on spot market prices in Germany, *Energy Policy* 36 (8) (2008) 3086–3094. doi:10.1016/j.enpol.2008.03.035.
- [15] M. Fleschutz, A. Leippi, M. Bohlayer, M. Braun, M. D. Murphy, Industrial grid fees vs. demand response: A case study of a multi-use battery in a German chemical plant, in: 2022 18th International Conference on the European Energy Market (EEM), IEEE, 2022, pp. 1–6. doi:10.1109/EEM54602.2022.9921156.
- [16] H. U. Buhl, Industrial flexibility options and their applications in a future energy system. White paper (2021). doi:10.24406/fit-n-639062.
- [17] M. Hamwi, I. Lizarralde, J. Legardeur, Demand response business model canvas: A tool for flexibility creation in the electricity markets, *Journal of Cleaner Production* 282. doi:10.1016/j.jclepro.2020.124539.
- [18] W. Huang, N. Zhang, C. Kang, M. Li, M. Huo, From demand response to integrated demand response: review and prospect of research and application, *Protection and Control of Modern Power Systems* 4 (1). doi:10.1186/s41601-019-0126-4.
- [19] R. Li, A. J. Satchwell, D. Finn, T. H. Christensen, M. Kummert, J. Le Dréau, R. A. Lopes, H. Madsen, J. Salom, G. Henze, K. Wittchen, Ten questions concerning energy flexibility in buildings, *Building and Environment* 223 (August) (2022) 109461. doi:10.1016/j.buildenv.2022.109461.
- [20] N. Lashmar, B. Wade, L. Molyneaux, P. Ashworth, Energy Research & Social Science Motivations, barriers, and enablers for demand response programs: A commercial and industrial consumer perspective, *Energy Research & Social Science* 90 (2022) 102667. doi:10.1016/j.erss.2022.102667.
- [21] T. Muche, C. Höge, O. Renner, R. Pohl, Profitability of participation in control reserve market for biomass-fueled combined heat and power plants, *Renewable Energy* 90 (2016) 62–76. doi:10.1016/j.renene.2015.12.051.
- [22] J. Wang, F. Wen, K. Wang, Y. Huang, Y. Xue, Optimal Operation of Commercial Buildings with Generalized Demand Response Management, in: A. Sharma, Q. Hao (Eds.), *International Conference on Innovative Smart Grid Technologies (ISGT Asia 2018)*, IEEE, Piscataway, NJ, 2018, pp. 265–270. doi:10.1109/ISGT-Asia.2018.8467984.
- [23] M. T. Kelley, R. C. Pattison, R. Baldick, M. Baldea, An MILP framework for optimizing demand response operation of air separation units, *Applied Energy* 222 (2018) 951–966. doi:10.1016/j.apenergy.2017.12.127.
- [24] S. Scholz, F. Meisel, Coordination of heterogeneous production equipment under an external signal for sustainable energy, *Journal of Cleaner Production* 338 (2022) 130461. doi:10.1016/j.jclepro.2022.130461.
- [25] D. L. Summerbell, D. Khripko, C. Barlow, J. Hesselbach, Cost and carbon reductions from industrial demand-side management: Study of potential savings at a cement plant, *Applied Energy* 197 (2017) 100–113. doi:10.1016/j.apenergy.2017.03.083.
- [26] T. M. Alabi, L. Lu, Z. Yang, A novel multi-objective stochastic risk co-optimization model of a zero-carbon multi-energy system (ZCMES) incorporating energy storage aging model and integrated demand response, *Energy* 226 (2021) 120258. doi:10.1016/j.energy.2021.120258.
- [27] A. Ahmarinejad, A Multi-objective Optimization Framework for Dynamic Planning of Energy Hub Considering Integrated Demand Response Program, *Sustainable Cities and Society* 74 (June) (2021) 103136. doi:10.1016/j.scs.2021.103136.
- [28] I. Petkov, P. Gabrielli, Power-to-hydrogen as seasonal energy storage: an uncertainty analysis for optimal design of low-carbon multi-energy systems, *Applied Energy* 274 (2020) 115197. doi:10.1016/j.apenergy.2020.115197.
- [29] S. A. Mansouri, A. Ahmarinejad, F. Sheidaei, M. S. Javadi, A. Rezaee Jordehi, A. Esmaeel Nezhad, J. P. Catalão, A multi-stage joint planning and operation model for energy hubs considering integrated demand response programs, *International Journal of Electrical Power and Energy Systems* 140 (2022) 108103. doi:10.1016/j.ijepes.2022.108103.
- [30] M. R. Cremi, A. M. Pantaleo, K. H. van Dam, N. Shah, Optimal design and operation of an urban energy system applied to the Fiera Del Levante exhibition centre, *Applied Energy* 275 (2020) 115359. doi:10.1016/j.apenergy.2020.115359.
- [31] N. Baumgärtner, R. Delorme, M. Hennen, A. Bardow, Design of low-carbon utility systems: Exploiting time-dependent grid emissions for climate-friendly demand-side management, *Applied Energy* 247 (2019) 755–765. doi:10.1016/j.apenergy.2019.04.029.
- [32] A. R. Jordehi, Optimisation of demand response in electric power systems, a review, *Renewable and Sustainable Energy Reviews* 103 (2019) 308–319. doi:10.1016/j.rser.2018.12.054.
- [33] Z. Luo, J. Peng, J. Cao, R. Yin, B. Zou, Y. Tan, J. Yan, Demand Flexibility of Residential Buildings: Definitions, Flexible Loads, and Quantification

Methods, Engineering 16 (2022) 123–140. doi:10.1016/j.eng.2022.01.010.

[34] L. Zhang, N. Good, P. Mancarella, Building-to-grid flexibility: Modelling and assessment metrics for residential demand response from heat pump aggregations, Applied Energy 233-234 (June 2018) (2019) 709–723. doi:10.1016/j.apenergy.2018.10.058.

[35] H. Li, H. Johra, F. d. A. Pereira, T. Hong, J. L. Dreau, A. Maturo, M. Wei, Y. Liu, A. Saberi-Derakhtenjani, Z. Nagy, A. Marszal-Pomianowska, D. Finn, S. Miyata, K. Kaspar, K. Nweye, Z. O. Neill, F. Pallonetto, B. Dong, Data-driven key performance indicators and datasets for building energy flexibility: A review and perspectives doi:10.48550/ARXIV.2211.12252.

[36] M. Joung, J. Kim, Assessing demand response and smart metering impacts on long-term electricity market prices and system reliability, Applied Energy 101 (2013) 441–448. doi:10.1016/j.apenergy.2012.05.009.

[37] L. Hirth, The optimal share of variable renewables: How the variability of wind and solar power affects their welfare-optimal deployment, Energy Journal 36 (1) (2015) 149–184. doi:10.5547/01956574.36.1.6.

[38] W. Zappa, M. Junginger, M. van den Broek, Can liberalised electricity markets support decarbonised portfolios in line with the Paris Agreement? A case study of Central Western Europe, Energy Policy 149 (January 2020) (2021) 111987. doi:10.1016/j.enpol.2020.111987.

[39] C. Yang, B. He, H. Liao, J. Ruan, J. Zhao, Price-based low-carbon demand response considering the conduction of carbon emission costs in smart grids, Frontiers in Energy Research 10 (August) (2022) 1–12. doi:10.3389/fenrg.2022.959786.

[40] M. Fleschutz, DrafProject/DRAF: v0.3.0 (Jan 2023). doi:10.5281/zenodo.7537745.

[41] M. Fleschutz, M. Bohlayer, M. Braun, M. D. Murphy, Demand Response Analysis Framework (DRAF): An Open-Source Multi-Objective Decision Support Tool for Decarbonizing Local Multi-Energy Systems, Sustainability 14 (13) (2022) 8025. doi:10.3390/su14138025.

[42] M. Fleschutz, M. Murphy, elmada: Dynamic electricity carbon emission factors and prices for Europe, Journal of Open Source Software 6 (66) (2021) 3625. doi:10.21105/joss.03625.

[43] V. Quaschnig, Regenerative Energiesysteme: Technologie – Berechnung – Klimaschutz, 10th Edition, 2019.

[44] M. Fleschutz, M. Bohlayer, M. Braun, G. Henze, M. D. Murphy, The effect of price-based demand response on carbon emissions in european electricity markets: The importance of adequate carbon prices, Applied Energy 295 (2021) 117040. doi:10.1016/j.apenergy.2021.117040.

[45] buzer, Annex 9 German Buildings Energy Act GEG: Conversion into greenhouse gas emissions. URL https://www.buzer.de/Anlage_9_GEG.htm

[46] ASUE, BHKW-Kenndaten 2011. URL <https://perma.cc/KHG2-WPPX>

[47] Viessmann, Preisliste DE Heizsysteme. URL <https://perma.cc/U2JM-R2L7>

[48] R. Hinterberger, J. Hinrichsen, S. Dedeyne, Power-To-Heat Anlagen zur Verwertung von EEÜberschussstrom – neuer Rechtsrahmen im Energiewirtschaftsgesetz, bisher ohne Wirkung. URL <https://perma.cc/FF2E-SE33>

[49] E. Vartiainen, G. Masson, C. Breyer, D. Moser, E. R. Medina, Impact of weighted average cost of capital, capital expenditure, and other parameters on future utility-scale PV levelised cost of electricity, Progress in Photovoltaics: Research and Applications 28 (6) (2019) 439–453. doi:10.1002/pip.3189.

[50] WindEurope, Europe invested €41bn in new wind farms in 2021. URL <https://perma.cc/59W7-Y9DN>

[51] J. Figgner, P. Stenzel, K.-P. Kairies, J. Linßen, D. Haberschusz, O. Wesels, M. Robinius, D. Stolten, D. U. Sauer, The development of stationary battery storage systems in germany – status 2020, Journal of Energy Storage 33 (2021) 101982. doi:10.1016/j.est.2020.101982.

[52] FFE, Verbundforschungsvorhaben Merit Order der Energiespeicherung im Jahr 2030. URL <https://perma.cc/F9X5-HG3B>

[53] E. Redondo-Iglesias, P. Venet, S. Pelissier, Measuring reversible and irreversible capacity losses on lithium-ion batteries, in: 2016 IEEE Vehicle Power and Propulsion Conference (VPPC), IEEE, 2016. doi:10.1109/vppc.2016.7791723.

[54] M. Bohlayer, G. Zöttl, Low-grade waste heat integration in distributed

energy generation systems - An economic optimization approach, Energy 159 (2018) 327–343. doi:10.1016/j.energy.2018.06.095.

[55] C. Plumley, Kelmarsh wind farm data (2022). doi:10.5281/ZENODO.5841834.

[56] A. Leippi, M. Fleschutz, M. D. Murphy, A review of ev battery utilization in demand response considering battery degradation in non-residential vehicle-to-grid scenarios, Energies 15 (9). doi:10.3390/en15093227.

[57] M. Fasihi, O. Efimova, C. Breyer, Techno-economic assessment of CO2 direct air capture plants, Journal of Cleaner Production 224 (2019) 957–980. doi:10.1016/j.jclepro.2019.03.086.

Appendix A. Detailed results

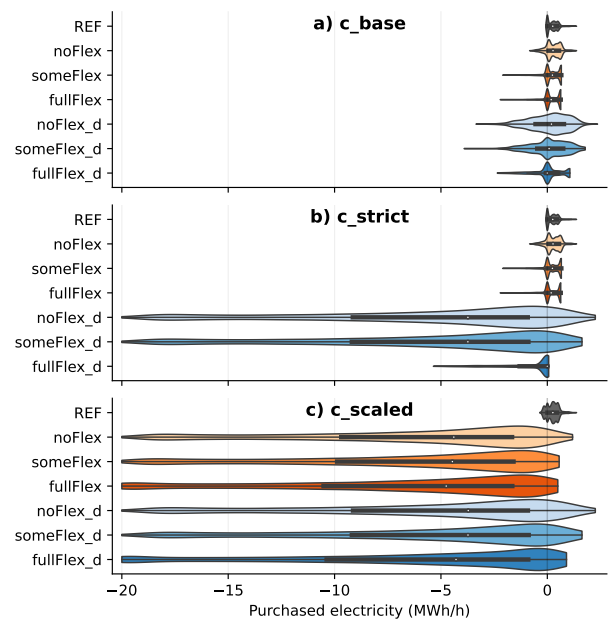


Fig. A.22. Violin plot of purchased (+) and sold (-) electricity.

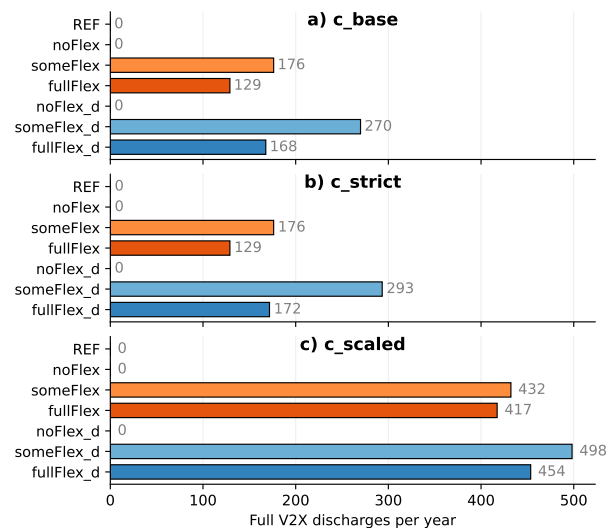


Fig. A.23. Number of full V2X discharges per year of average BEV battery (i.e. total annual energy V2X discharge divided by the usable battery capacity).

Table A.4

Nominal capacities of new technologies in kW or kWh (see base unit of Table 1). Colors highlight differences between scenarios. All-zero columns were removed.

	c_base					c_strict					c_scaled										
	HP	P2H	PV	TES	WT	BES	Elc	FC	H2S	HP	P2H	PV	TES	WT	BES	HP	P2H	PV	TES	WT	
REF	0	0	0	0	0	0	0	0	0	0	0	0	0	0	0	0	0	0	0	0	0
noFlex	918	105	1,356	0	0	0	0	0	0	918	105	1,356	0	0	0	907	314	3,077	0	0	18,982
someFlex	907	197	2,853	0	0	0	0	0	0	907	197	2,853	0	0	0	907	485	3,077	0	0	19,492
fullFlex	760	222	3,028	3,216	0	0	0	0	0	760	222	3,028	3,216	0	14	757	1,414	3,077	8,986	20,875	
noFlex_d	1,723	485	3,077	0	2,183	0	0	0	0	1,639	567	3,077	0	19,413	0	1,546	659	3,077	0	19,413	
someFlex_d	1,049	863	3,077	0	2,140	0	0	0	0	1,106	716	3,077	0	19,492	0	1,045	872	3,077	0	19,492	
fullFlex_d	899	1,082	3,077	14,675	2,344	169	456	804	189,953	969	1,592	3,077	27,807	5,347	18	1,085	2,214	3,077	22,060	21,859	

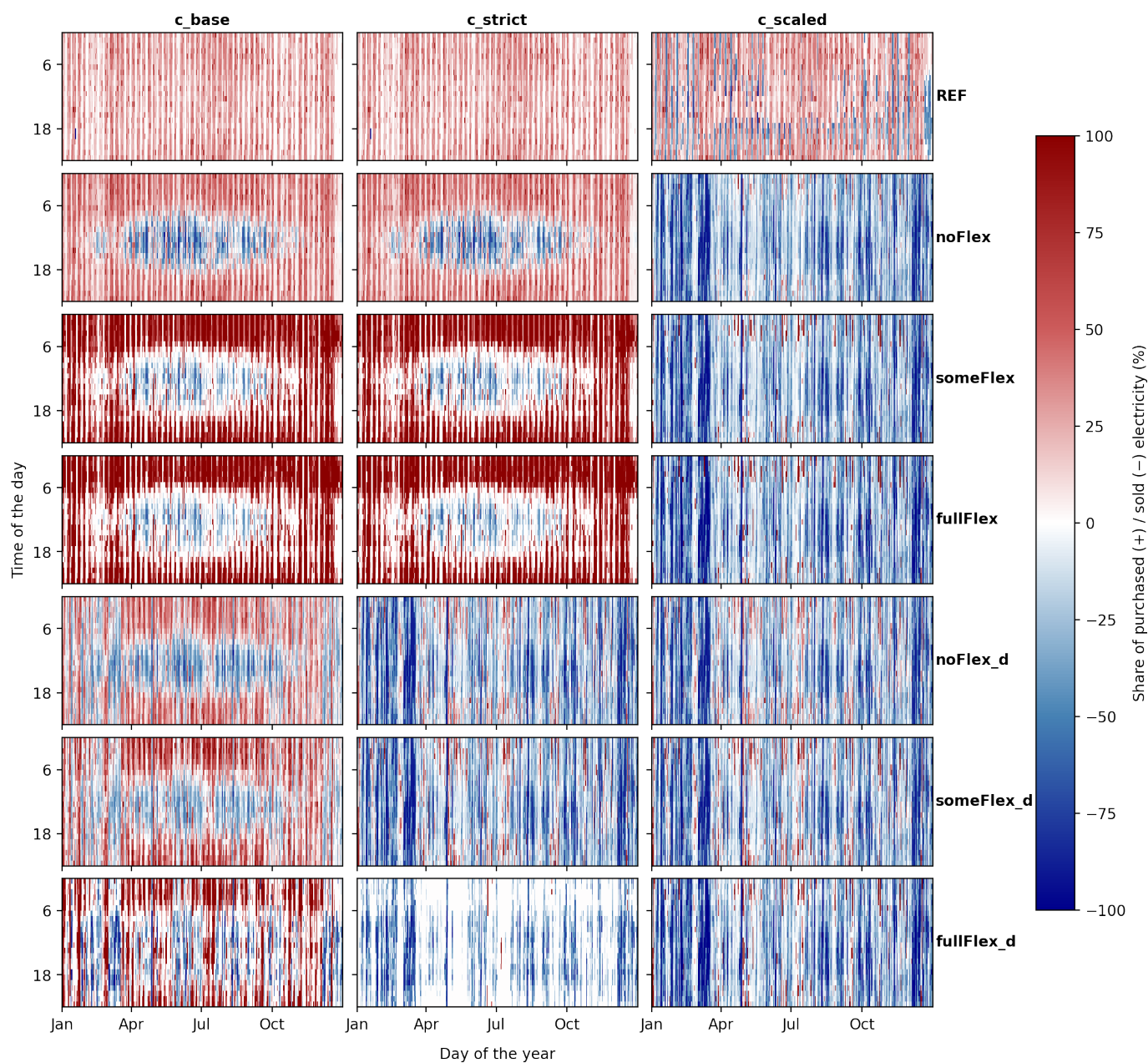


Fig. A.24. Heatmaps of purchased (+) and sold (-) electricity in % based on maximum purchased and sold electricity, respectively.

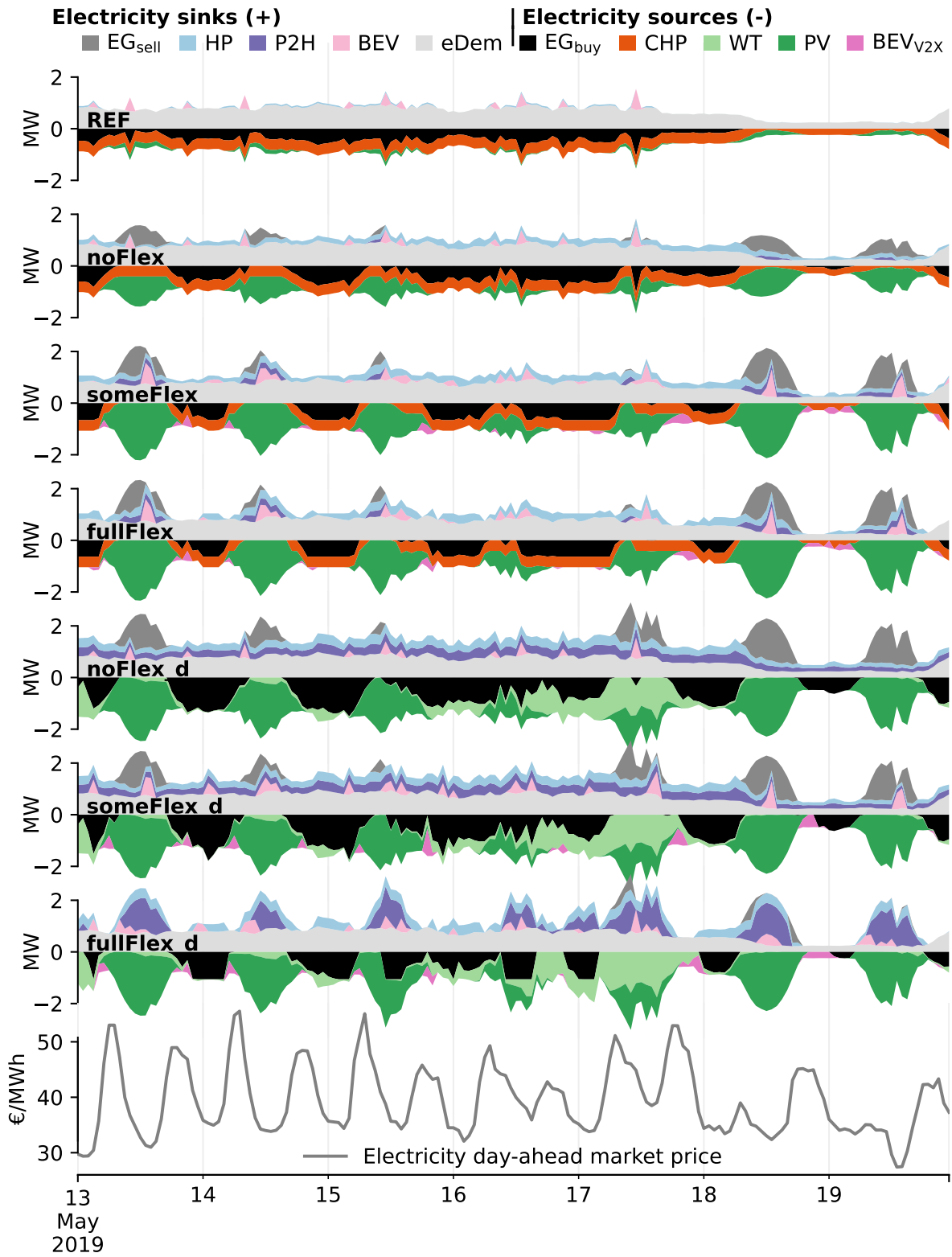


Fig. A.25. Electricity balance of the c_base context for one week (Monday–Sunday) in May 2019.

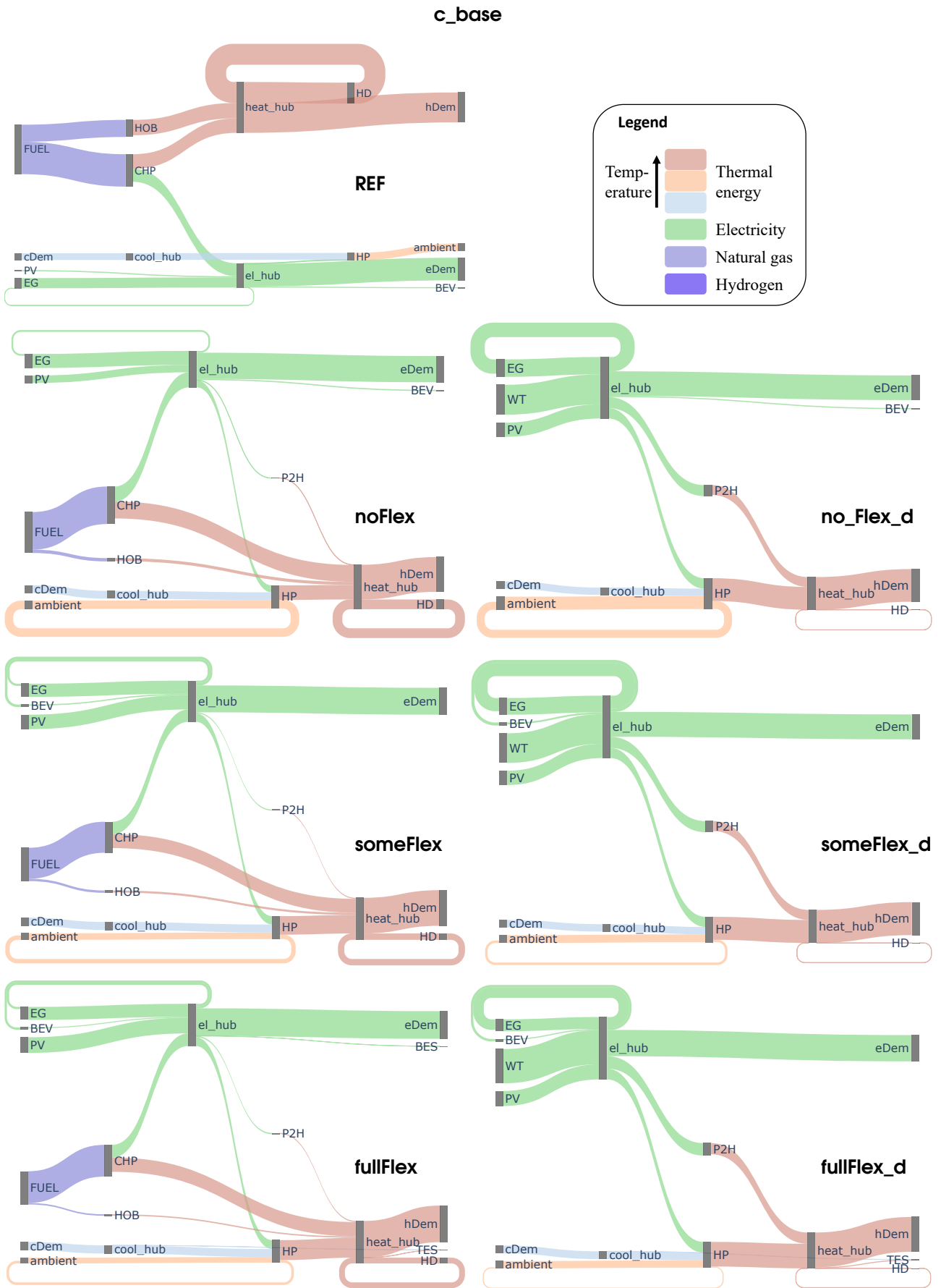


Fig. A.26. Sankey diagrams of annual energy sums for the c_base context.

c_strict

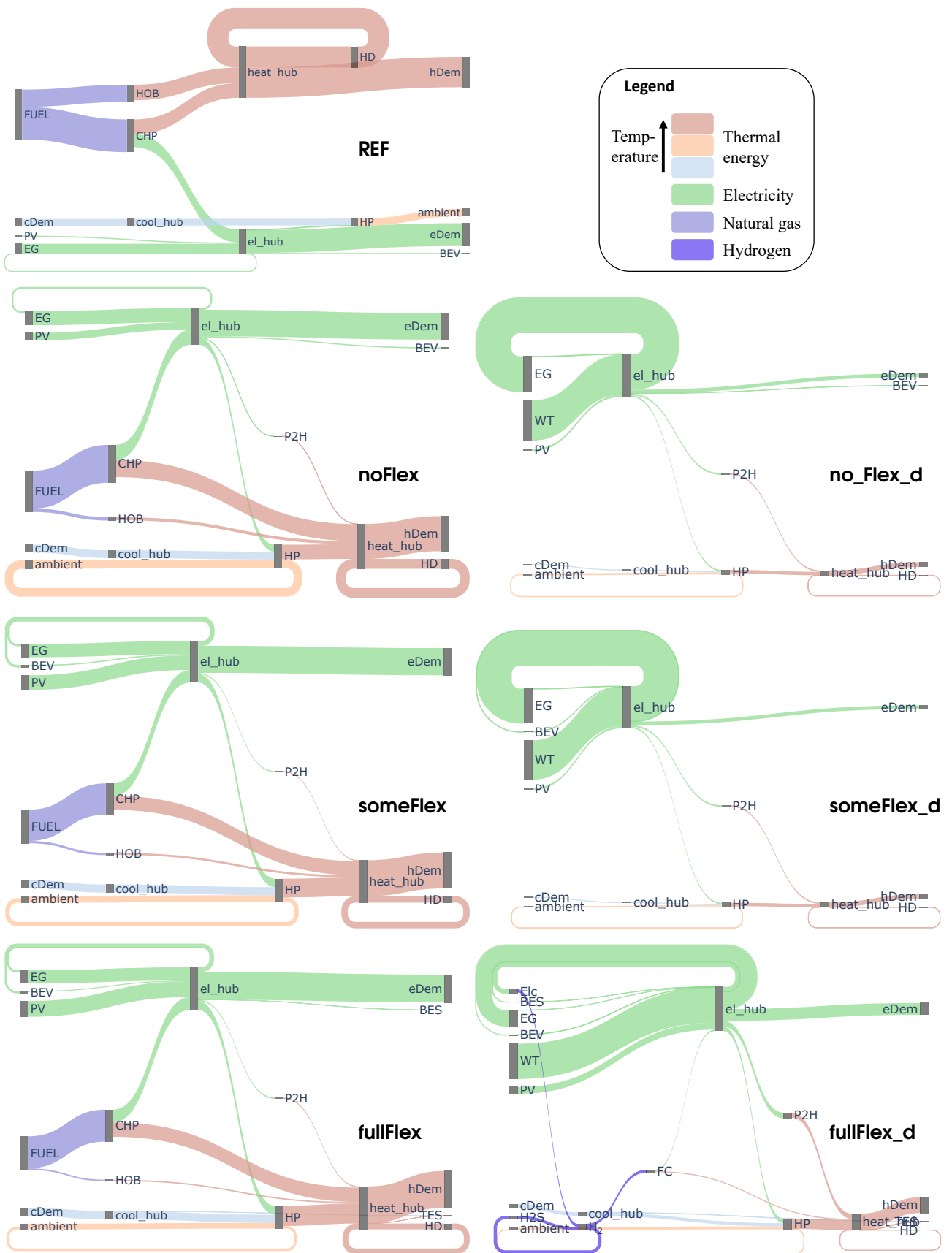


Fig. A.27. Sankey diagrams of annual energy sums for the c_strict context.

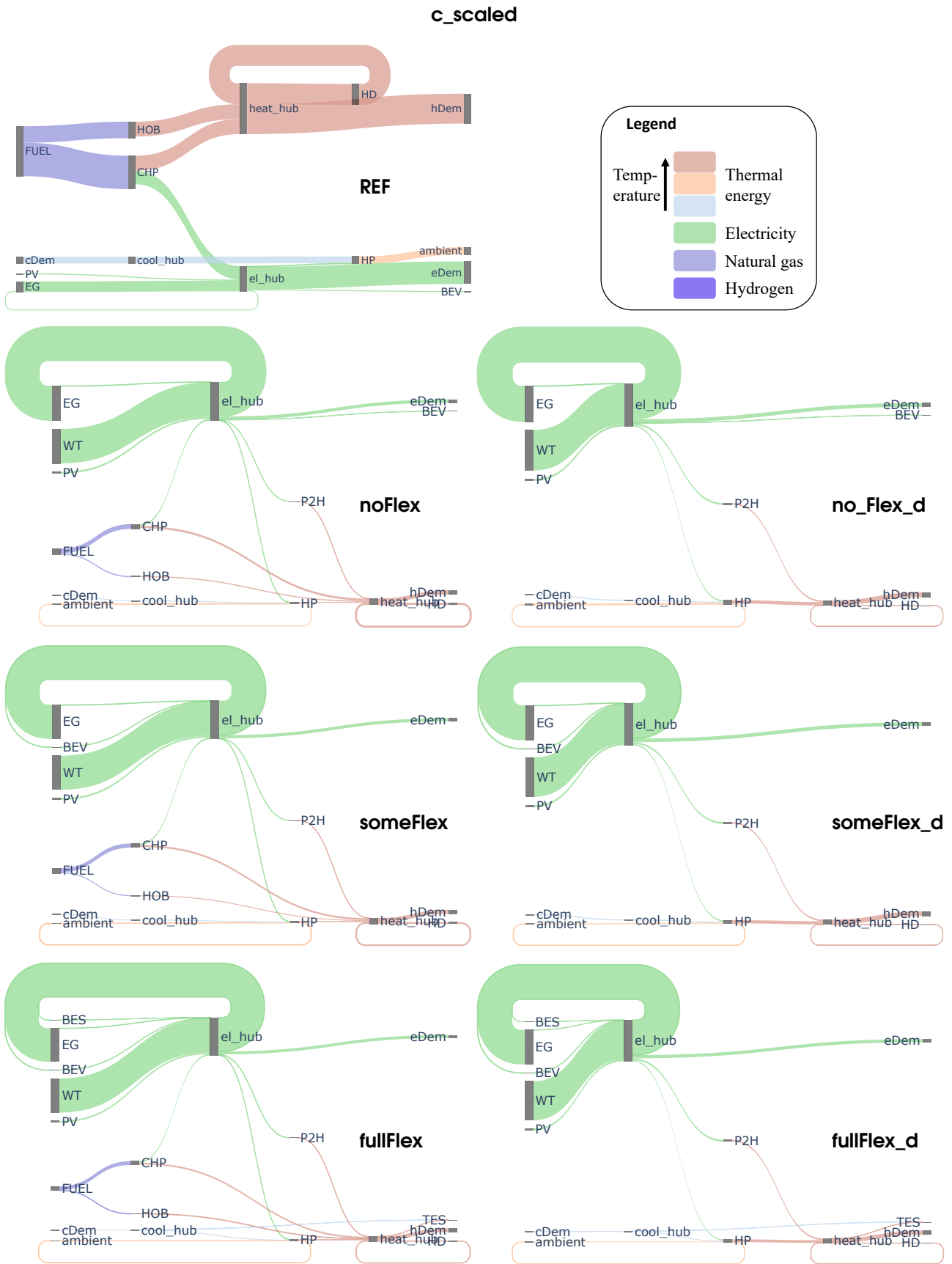


Fig. A.28. Sankey diagrams of annual energy sums for the **c_scaled** context.